Received: 28 February 2022 | Revised: 3 January 2023 | Accepted: 27 January 2023

DOI: 10.1111/gbi.12550

gebiology WILEY

ORIGINAL ARTICLE

Ediacaran–Cambrian bioturbation did not extensively oxygenate sediments in shallow marine ecosystems

Alison T. Cribb[1] | Sebastiaan J. van de Velde[2,3] | William M. Berelson[1] | David J. Bottjer[1] | Frank A. Corsetti[1]

[1]Department of Earth Sciences, University of Southern California, Los Angeles, California, USA

[2]Department of Geosciences, Environment and Society, Universté Libre de Bruxelles, Brussels, Belgium

[3]Operational Directorate Natural Environment, Royal Belgian Institute of Natural Sciences, Brussels, Belgium

Correspondence
Alison T. Cribb, Department of Earth Sciences, University of Southern California, Los Angeles, CA, USA.
Email: cribb@usc.edu

Abstract

The radiation of bioturbation during the Ediacaran–Cambrian transition has long been hypothesized to have oxygenated sediments, triggering an expansion of the habitable benthic zone and promoting increased infaunal tiering in early Paleozoic benthic communities. However, the effects of bioturbation on sediment oxygen are underexplored with respect to the importance of biomixing and bioirrigation, two bioturbation processes which can have opposite effects on sediment redox chemistry. We categorized trace fossils from the Ediacaran and Terreneuvian as biomixing or bioirrigation fossils and integrated sedimentological proxies for bioturbation intensity with biogeochemical modeling to simulate oxygen penetration depths through the Ediacaran–Cambrian transition. Ultimately, we find that despite dramatic increases in ichnodiversity in the Terreneuvian, biomixing remains the dominant bioturbation behavior, and in contrast to traditional assumptions, Ediacaran–Cambrian bioturbation was unlikely to have resulted in extensive oxygenation of shallow marine sediments globally.

1 | INTRODUCTION

The evolution of bioturbation during the Ediacaran Period and subsequent radiation of complex burrowing behaviors during the Paleozoic Era is one of the most important geobiological transitions in Earth history, as it fundamentally changed the nature of the sediment–water interface and the structure of benthic ecosystems. During the Ediacaran, shallow marine (broadly defined as marine ecosystems above the ocean shelf break) sediments are thought to have been predominantly anoxic with a very shallow oxic–anoxic interface due to being unbioturbated, as well as often covered in microbial mats that are thought to have sealed the sediment from oxygen exchange between porewaters and the overlying water column (Seilacher & Pflüger, 1994). Then, in the early Cambrian, as the diversity of bioturbation behaviors radiated in shallow marine environments (Buatois & Mángano, 2018), the sediment tiers where animals predominantly lived are thought to have become increasingly oxygenated due to burrowing macrofauna disrupting the microbial mats, stimulating oxygen diffusion into the sediment, and, critically, by actively mixing oxygen into the sediments themselves via bioturbation (Savrda & Bottjer, 1991; Seilacher, 1999). It has been proposed that the bioturbation-driven oxygenation of the sediment further promoted more infaunal activity, creating a positive bioturbation-oxygen feedback loop until the shallow seafloor was colonized by infauna and fully bioturbated in the Early Paleozoic (McIlroy & Logan, 1999). Well-bioturbated sediments, represented by ichnofabrics with fully disrupted sediment laminae, have been observed in the lower Cambrian (Gougeon et al., 2018) and are traditionally assumed to imply seafloors into which oxygen vertically penetrated (Savrda & Bottjer, 1991), although it remains unclear whether or not deeper sediment tiers would have been extensively oxygenated. Nevertheless, it has been suggested that the radiation

of bioturbators during the Ediacaran–Cambrian transition drove an expansion in habitability of the shallow to deep sediment tiers (Mángano & Buatois, 2020), largely due to increased sediment oxygenation resulting from the disappearance of microbial mats and the early evolution of oxygenating bioturbation behaviors (McIlroy & Logan, 1999; Tarhan, 2018a). However, the extent to which the evolution of new and more intense bioturbation behaviors during the Ediacaran–Cambrian transition might have influenced oxygen penetration into the sediment – which broadly describes the thickness of the sedimentary oxic zone before oxygen concentrations fall to zero (Cai & Sayles, 1996) – and the habitability of the sediments for aerobic infaunal animals has been underexplored using quantitative methods.

While bioturbation broadly refers to any biogenic sediment mixing, bioturbation behaviors can be more precisely divided into which phase of the sediment is being mixed (Kristensen et al., 2012). Previous work has demonstrated that biomixing (bioturbation behaviors which mix the sediment solid-phase particles) and bioirrigation (those which enhance the exchange of solutes between the porewater and the overlying water) can have opposite effects on the fate of oxygen in the sediment (Aller, 1982; Kristensen et al., 2012; van de Velde & Meysman, 2016). Biomixing ultimately restricts the depth of the oxic zone in the sediment primarily by transporting more organic matter below the oxic–anoxic interface to stimulate anaerobic respiration, producing reduced compounds that are eventually oxidized, thus contributing to the consumption of oxygen deeper in the sediment. In contrast, bioirrigation increases oxygen concentrations in deeper sediment tiers by supplying more oxygen to the sediment depth via burrow flushing with oxygenated waters from the overlying water column (van de Velde & Meysman, 2016). Previously proposed biogeochemical and paleoecological effects of the evolution of bioturbation are underexplored with respect to the contrasting effects of biomixing and bioirrigation on sediment redox chemistry (Boyle et al., 2014; Canfield & Farquhar, 2009; Tarhan et al., 2015).

Here, we investigate whether early bioturbators in the Ediacaran and Terreneuvian could have feasibly oxygenated sediments in shallow marine environments to increase the habitability of deeper sediment tiers for aerobic macroinfauna, considering the record of biomixing and bioirrigation in the trace fossil record (Buatois et al., 2020) and by integrating sedimentological bioturbation intensity proxies with a sedimentary biogeochemical reaction-transport model. Specifically, we simulate the oxygen penetration depth (OPD, or the minimum one-dimensional sediment depth at which $[O_{2,BW}] < 1$ μmol) by using data from the trace fossil record to parameterize biomixing and bioirrigation intensities in the model. We also investigate the impact of different bioturbation intensities on oxygen consumption rates and reactions to mechanistically understand why different bioturbation parameters lead to different effects on the OPD. Henceforth, we refer to bioturbation as meaning biomixing and bioirrigation operating together and to biomixing and bioirrigation as each behavior operating independently. Note that here we explore the sole impact of bioturbation on the OPD, rather than the combined role of bioturbators and the break-up of microbial mats. In addition to the differential impact of biomixing versus bioirrigation (van de Velde & Meysman, 2016), extrinsic environmental factors also likely had a significant, and perhaps competing, impact on oxygen penetration into the sediment during the Ediacaran and well into the Paleozoic. Specifically, oxygen concentrations in the ocean and organic matter dynamics changed around the time of increases in bioturbation intensity and bioturbator size (Dahl et al., 2019; Fakhraee et al., 2020; Lu et al., 2018; Lyons et al., 2014; van de Velde et al., 2018), which would have also impacted the extent of oxygen penetration into the sediment, particularly as organic matter dynamics are typically the driving force of sediment oxygen dynamics in today's ocean (Cai & Sayles, 1996; Kristensen, 2000). Organic matter delivery to the seafloor may also impact oxygen penetration into the sediment indirectly by influencing the physiology, activity, and abundances of bioturbators (Smith et al., 1997; Sperling & Stockey, 2018). Thus, we also investigate the importance of organic matter flux and its potentially competing or synergistic relationship with bioturbation on oxygen penetration into the sediment.

2 | METHODS

We investigated two components of the Ediacaran–Cambrian trace fossil record to test the hypothesis that the evolution of new bioturbation behaviors through the Ediacaran–Cambrian transition resulted in macrofauna-driven oxygenation of shallow marine sediments. First, we quantified the proportion of biomixers to bioirrigators and any changes in the relative abundance of the two behaviors across the Ediacaran–Cambrian boundary. To achieve this, we used a previously compiled global trace fossil dataset (Buatois et al., 2020) and classified each ichnogenus as a biomixing or bioirrigation behavior. This record of biomixing and bioirrigation serves as important context from the fossil record in which our model can be grounded and addresses previous hypotheses that bioirrigators were the dominant bioturbation ecosystem engineering behavior in early Cambrian ecosystems (McIlroy & Logan, 1999; Tarhan, 2018a). Second, we compiled sedimentological proxies of bioturbation intensity to parameterize biodiffusion and bioirrigation coefficients. Specifically, we compiled global average mixed layer depths and Bioturbation Index (BI) values and converted them to biodiffusion and bioirrigation coefficients, which were then integrated with a biogeochemical reaction-transport model. We developed a one-dimensional reaction-transport model simulating carbon, oxygen, nitrogen, and sulfur cycling. We have omitted iron and manganese reactions from our model for sake of computational simplicity and efficiency in our modeling experiments and sensitivity analyses, although we have run a subset of our analyses in a more geochemically comprehensive and complex reaction-transport model (Zhao et al., 2020) to compare results.

Using this reaction-transport model, we conducted two types of analyses. First, in three different types of experiments, we simulated the OPD at various bottom-water oxygen concentrations

and organic matter fluxes at different bioturbation intensities to investigate (1) the broad impacts of early bioturbation on the OPD and (2) the sensitivity of those impacts to bottom-water oxygen and organic matter dynamics. Second, we simulated the pathways of total oxygen consumption in the sediment in order to investigate why different levels of bioturbation intensity and types of bioturbation have potentially opposite impacts on the fate of oxygen in the sediment. For each analysis, we simulated results with no bioturbation, Ediacaran bioturbation parameters, Terreneuvian bioturbation parameters, and modern bioturbation parameters.

2.1 | Trace fossil dataset and bioturbation parameterization

The trace fossil dataset used here (Data S1) is primarily from Buatois et al. (2020). Ediacaran (Vendian and Nama) and Terreneuvian (Fortunian and Cambrian Stage 2) trace fossils were selected from the larger dataset. Some Ediacaran ichnogenera which were not originally included – such as *Planolites* (Corsetti & Hagadorn, 2000) and *Lamonte* (Meyer et al., 2014; O'Neil et al., 2020) – were added to the dataset along with their stratigraphic occurrences. Trace fossils were then classified as either biomixers or bioirrigators at the ichnogenus level based on feeding behavior and burrow architecture, both of which are given for each ichnogenus in Buatois et al. (2020). We follow previous interpretations (Herringshaw et al., 2017; Kristensen et al., 2012) that primarily vertically oriented suspension feeding and predator ichnogenera represent bioirrigation, while primarily horizontally oriented deposit feeding and predatory ichnogenera represent biomixing. As a caveat, we note that semi-permanent or permanent burrows constructed by suspension feeders necessarily result in some redistribution of sediment particles, and thus, bioirrigation is unlikely to occur without some biomixing. However, the effects of bioirrigation and biomixing will primarily be considered together in the following results. Ichnogenera that represent surficial scratches, trackways, and imprints were removed, as they represent surficial modification that results in negligible sediment mixing (Herringshaw et al., 2017). From the final trace fossil dataset, we calculated two relative abundance metrics: the relative abundance of biomixing and bioirrigation behaviors first from total unique ichnogenera and second from unique stratigraphic occurrences (as they were given in the original dataset; Buatois et al., 2020). These metrics are akin to ichnodiversity and ichnoabundance, respectively. The resulting trace fossil data of biomixers and bioirrigators were not directly incorporated into the models presented here, as the biodiffusion and bioirrigation coefficients were derived from sedimentological proxies of sediment mixing. However, the trace fossil record of biomixing and bioirrigation serves as an important conceptual comparison between the modeled results and the preserved evolutionary history of bioturbation. For example, if the dominance of biomixers or bioirrigators changed across the Ediacaran–Cambrian boundary, one might imagine that the resulting biogeochemical impacts unique to biomixing or bioirrigation would have also changed across the Ediacaran–Cambrian boundary.

Average mixed layer depths (x_L) from Tarhan et al. (2015) and Bioturbation Index (BI) values from Mángano and Buatois (2014) were used to calculate biodiffusion coefficients as they relate to the mixed layer depth. For the Bioturbation Index, which measures the vertical disruption of ichnofabrics (Taylor & Goldring, 1993), BI values were normalized to x_L by assuming the average mixed layer depth, x_L = 10 cm (Boudreau, 1998), correlates to BI = 6, the maximum Bioturbation Index (BI) value (see Tarhan et al., 2015 for similar normalization of modern ichnofabric index (ii) (Droser & Bottjer, 1986) values to mixed layer depths). Mixed layer depths were then converted to biodiffusion coefficients using two different relationships. First, we use the biomixing-mixed layer depth relationship described in van de Velde and Meysman (2016),

$$x_L = x_{L,0} + x_{L,\max}\left(1 - \exp\left(-D_{B,0}/D_{B,ref}\right)\right),$$

where $x_{L,0}$ is the minimum depth of bioturbation (0.1 cm), $x_{L,\max}$ is the maximum depth of bioturbation ($x_{L,0}+x_{L,\max}$ = 10 cm; Boudreau, 1998; van de Velde & Meysman, 2016), and $D_{B,\mathrm{ref}}$ is the reference biomixing intensity for coastal sediments ($D_{B,\mathrm{ref}}$ = 3 cm^2 year^{-1}; Boudreau, 1998; van de Velde & Meysman, 2016). We also used the biomixing-mixed layer depth relationship described by Boudreau (1998) to calculate a second biodiffusion coefficient,

$$x_L = 4\sqrt{9 * \frac{D_{B,0}}{8k}},$$

where k is the organic matter reactivity. In the following models, we used a refractory organic matter value of k = 0.1 year^{-1} and a labile organic matter value of k = 10 year^{-1}. The flux of both fractions of organic matter is equal, so we calculated an average k-value of 5 year^{-1} for bulk organic matter at the sediment–water interface. We used the k = 5 year^{-1} to calculate biodiffusion coefficients at the sediment–water interface ($D_{B,0}$). The biodiffusion coefficients ultimately used are the average of the biodiffusion coefficients calculated via these two different methods. Finally, we note that although other BI and ichnofabric index (ii) values are reported as local maxima for Ediacaran and Terreneuvian localities, we emphasize that we do not use local maxima mixed layer depths, BI values, or ii values, as very localized intense bioturbation can occur which does not necessarily represent the entire marine environment's nor the global average sediment mixing (Tarhan, 2018a). Finally, we used modern biodiffusion coefficients to serve as end-member comparison results. We used a modern global averaged biodiffusion coefficient, which describes biomixing intensity, of 10 cm^2 year^{-1} (based on modern data quantified using the ^{210}Pb method; Lecroart et al., 2010; Solan et al., 2019). Bioirrigation rates are more difficult to quantify, but diagenetic models tend to use a modern bioirrigation coefficient around 365 year^{-1} (van de Velde & Meysman, 2016). We note, however, these modern biodiffusion and bioirrigation coefficients that have been selected only represent a

subset of modern bioturbation intensities, which vary quite extensively in the modern ocean, particularly in response to water depth, net primary productivity, season, and climate (Solan et al., 2019).

2.2 | Reaction-Transport model formulation

We developed a one-dimensional reaction-transport model to simulate carbon, oxygen, nitrogen, and sulfur cycling in a sediment column. The reaction-transport model was developed using the R package CRAN:ReacTran (Soetaert & Meysman, 2012), which is formulated from two coupled mass balance equations for solids and solutes in the model sediment column (Boudreau, 1997; Meysman et al., 2005):

$$\begin{cases} \varphi\frac{\partial C_i}{\partial t} = \frac{\partial}{\partial z}\left(\varphi D_i\frac{\partial C_i}{\partial z} - \varphi v C_i\right) + \varphi\alpha(z)\left(C_{i,sw} - C_i(z)\right) + \sum_n v_{i,n}R_n \\ (1-\varphi)\frac{\partial S_i}{\partial t} = \frac{\partial}{\partial z}\left((1-\varphi)D_B(z)\frac{\partial S_i}{\partial z} - (1-\varphi)wS_i\right) + \sum_n v_{i,n}R_n \end{cases}$$

In these equations, C_i represents the concentration of solute species, S_i represents the concentration of solid species, z is the depth in the sediment column, and φ represents the porosity. The equation for the change in the concentration of solutes includes two transport processes: first, molecular advection and diffusion, following Fick's first law ($J_D = -\varphi D_i\frac{\partial C_i}{\partial z} + \varphi v C_i$; Fick, 1855), and second, bioirrigation transport ($I_{irr}(z) = \alpha(z)\left(C_{i,sw} - C_i(z)\right)$) (Boudreau, 1984; Emerson et al., 1984). For molecular advection and diffusion, D_i represents the molecular diffusion coefficients for each solute species as a function of temperature and salinity, which we calculate using the R package CRAN:marelac (Soetaert et al., 2020) and correct for tortuosity with the correction factor $\theta^2 = 1 - 2\ln(\varphi)$ (Boudreau, 1996), and v represents porewater sedimentation velocity in the compacted, impermeable sediment deposit. For bioirrigation transport, $\alpha(z)$ represents the bioirrigation coefficient at each sediment depth, $C_{i,\mathrm{SW}}$ is the solute concentration at the sediment–water interface, and $C_i(z)$ is the solute concentration at each sediment depth. The equation for the change in solids also includes two transport processes: first, biodiffusion transport ($D_B(z)\frac{\partial S_i}{\partial z}$), and second, advection due to sedimentation ($(1-\varphi)wS_i$). For biodiffusion transport, $D_B(z)$ is solid-phase sediment volume-based and represents the biodiffusion coefficients at each sediment depth. For advection due to sedimentation, w represents the solid-phase sedimentation velocity.

The concentrations of both solids and solutes are changed by production and consumption by biogeochemical reactions, expressed in each equation as $\sum_n v_{i,n}R_n$. Here, R_n represents the reaction rate for the nth reaction, and $v_{i,n}$ represents the stoichiometric coefficient for the ith species in the nth reaction. Seven reactions describe carbon, oxygen, nitrogen, and sulfur cycling (Table S1). The primary reactions are aerobic respiration, nitrate reduction, and sulfate reduction. The secondary oxidation reactions are canonical sulfide oxidation, ammonium oxidation, iron sulfide oxidation, and sulfide oxidation with nitrate. To account for a lack of full iron cycle to interact with hydrogen sulfide, a portion of hydrogen sulfide that is produced by sulfate reduction is precipitated as FeS. A full description of the biogeochemical reaction set, kinetic rate expressions, reaction rate expressions, and associated reaction constants are in Tables S1–S4. The model domain is a 15-cm sediment column parametrized to reflect fine-grained coastal sediments. For simplicity, we ignore compaction, so sediment porosity is constant with depth at $\varphi = 0.8$. Sedimentation velocity for solutes and solids is fixed at $v = w = 0.2$ cm year^{-1}, and the solid-phase sediment density (ρ) is 2.6 g cm^{-3}. Salinity (S) is 30, temperature (T) is 25°C, and pH is 7.5. All parameters are held constant through the model experiments. Full model parameters are described in Table S5. Finally, we again note that we omited Mn and Fe reactions from our model for the sake of computational simplicity, as adding additional complexity to this model would result in extended model solution times and lower oxygen profile resolution, although a subset of simulations was conducted using a more geochemically comprehensive reaction-transport model (Zhao et al., 2020).

Bioturbation is separated into and parameterized as biomixing and bioirrigation. Following convention, biomixing is described as a diffusive transport process or biodiffusion (Boudreau, 1997; Meysman et al., 2010). The biodiffusion coefficients $D_B(z)$ for each depth in the modeled sediment column follow a sigmoidal depth profile ($D_B(z) = D_{B,0}\exp\left(-\frac{(z-X_L)}{0.25x_{bm}}\right)/\left(1+\exp\left(-\frac{(z-X_L)}{0.25x_{bm}}\right)\right)$, where z is the sediment depth and x_{bm} is the depth attenuation coefficient for biomixing; Figure S1; Boudreau, 1998). Biodiffusion coefficients are given a sigmoidal profile because bioturbating benthic macrofauna are physiologically dependent on food and oxygen, which we assume are most available near the sediment–water interface. Thus, biomixing is most intense in the shallowest sediment tier and decreases with depth (Boudreau, 1998; Emerson et al., 1984). For simplicity, we ignore reactivity selection, particle size selection, and potential for differential transport in our biodiffusion coefficient profile. Bioirrigation is described as a non-local exchange process in which sediment porewater is exchanged with water at the sediment–water interface (Boudreau, 1984). Bioirrigation follows an exponential depth profile ($\alpha(z) = \alpha_0\exp\left(-\frac{z}{x_{\mathrm{irr}}}\right)$), where x_{irr} is the depth attenuation coefficient for bioirrigation (Figure S1; Kristensen et al., 2018; Martin & Banta, 1992). As with the depth dependency of biomixing, this equation also assumes that bioirrigation activity is most intense near the sediment–water interface, although instead follows an exponential profile (van de Velde & Meysman, 2016).

Finally, we note that here we use a non-local model for bioirrigation, which is a simplification of the complex, species-specific process of bioirrigation (Meile et al., 2005). We choose the one-dimensional non-local exchange model because more complex two- or three-dimensional models require assumptions about burrow structures, many of which cannot be validated based on the limited data available from the trace fossil record. Additionally, we apply one alpha for all solutes, meaning we ignore reactions at burrow walls (such as the oxidation of hydrogen sulfide at the edge of bioirrigated burrows). This ultimately means that the OPD simulations in bioirrigated cases should be viewed as conservative maximum results, as

reoxidation reactions at the burrow wall would limit the removal of hydrogen sulfide, leading to a higher oxygen consumption linked to sulfide oxidation. Thus, in reality, the OPDs for the bioirrigated experiments were likely shallower than the results presented here. We keep the alpha coefficient constant also due to the lack of solute-specific alpha values for global application, such as the results presented here.

2.3 | Modeling experiments and analyses

To investigate the sensitivity of the OPD to an increase in biomixing and bioirrigation intensity across the Ediacaran–Cambrian boundary, we simulated the OPD over a range of biodiffusion coefficients at four different oxygen levels. Biodiffusion coefficients were increased from $D_{B,0}$ = 0–3.0 cm^2 year^{-1} and bioirrigation coefficients were increased from α_0 = 0–300 year^{-1} at different bottom-water oxygen concentrations and organic matter fluxes. Bottom-water oxygen concentrations tested are $[O_{2,BW}]$ = 0.014 mM (5% PAL), 0.028 mM (10% PAL), 0.07 mM (25% PAL), 0.14 mM (50% PAL), 0.196 mM (70% PAL), and 0.28 mM (100% PAL), and organic matter fluxes tested are $CH_2O_{tot,F}$ = 150, 300, and 700 μmol cm^{-2} year^{-1}. Bottom-water oxygen concentrations have a fixed concentration, and organic matter fluxes have a constant steady delivery for this experiment and all further described model experiments. Sensitivity of the OPD to bioirrigation coefficients was tested with the chosen Ediacaran and Terreneuvian biodiffusion coefficients. Boundary conditions for these sensitivity analyses are given in Table S6. Second, to investigate the impact of different bioturbation intensities (both separately as biomixing or bioirrigation and as the two behaviors combined) over a large range of bottom-water oxygen concentrations and organic matter flux conditions, we conducted 10 modeling experiments that output simulated OPDs from $[O_{2,BW}]$ = 0.014–0.28 mM and the flux of total organic carbon from $CH_2O_{tot,F}$ = 100–450 μmol cm^2 year^{-1}. For oxygen, we focus specifically on $[O_{2,BW}]$ = 0.07–0.14 mM throughout the text, as a possible representation of 25%–50% PAL oxygen concentrations of the Ediacaran–Cambrian transition (Krause et al., 2018). For organic matter, we focus on fluxes in the range of 150–450 μmol cm^{-2} year^{-1}, which is within the low range of modern nearshore organic carbon flux estimates (Dunne et al., 2007) and encompasses previously used boundary conditions used to simulate early Paleozoic nearshore environments (Tarhan et al., 2021). Full boundary conditions for these analyses are given in Table S7. Where Ediacaran–Cambrian boundary conditions cannot be constrained based on available proxy information (e.g., temperature and salinity), we assume that boundary conditions from modern nearshore environments (Dale et al., 2015; Dunne et al., 2007; Mouret et al., 2009; van de Velde & Meysman, 2016) are appropriate. One experiment was run with no bioturbation as a control to compare the other nine experiments. The other nine experiments use bioturbation parameters for the Ediacaran, Terreneuvian, and modern. For each time interval, three experiments were run: one with only biomixing, one with only bioirrigation, and one with biomixing and bioirrigation together. For all experiments, 10,000 steady-state solutions were solved, representing the OPD simulated over 100 bottom-water oxygen concentrations and 100 organic matter fluxes. In order to more clearly visualize the role of organic matter flux and oxygen on the OPD as bioturbation evolved, from these larger analyses, the OPD was also plotted for organic matter fluxes at $CH_2O_{tot,F}$ = 100, 300, and 450 μmol cm^2 year^{-1} at two different end-member bottom-water oxygen concentrations for the Ediacaran–Cambrian transition, $[O_{2,BW}]$ = 0.07 and 0.14 mM. All boundary conditions are compiled for this experiment in Table S8. Finally, using our model outputs, we investigated the effect of bioturbation on oxygen consumption profile, specifically focusing on oxygen consumption via aerobic respiration and reoxidation pathways. We simulated reaction-rate profiles for oxygen consumption. Boundary conditions for this experiment are given in Table S9. We conducted 10 simulations for the same 10 different bioturbation intensity conditions consisting of no bioturbation, Ediacaran bioturbation, Terreneuvian bioturbation, and modern bioturbation parameters as the modeling experiments. We simulated total oxygen consumption, oxygen consumption via aerobic respiration, and oxygen consumption via reoxidation pathways. We also calculated burial of organic matter and iron sulfide. All models were constructed using the R package CRAN:ReacTran (Soetaert & Meysman, 2012), and all equations were solved to steady-state, which best represent geologic time scales, using the steady.1D function in the R package CRAN:rootSolve (Soetaert, 2009, Soetaert & Herman, 2009).

3 | RESULTS

3.1 | The Ediacaran–Cambrian trace fossil record of biomixing and bioirrigation intensity

There are a variety of both biomixing and bioirrigation ichnogenera in the Ediacaran and Terreneuvian trace fossil records. Common biomixing trace fossils in both the Ediacaran and Terreneuvian include small (sub-centimeter in diameter) horizontal *Helminthopsis*, *Helminthoidichnites*, and *Gordia* and typically larger (centimeter scale or larger in diameter) horizontal *Archaeonassa*, *Psammichnites*, *Palaeophycus*, and *Torrowangea* (Table 1). Predominantly vertical trace fossils that represent suspension and predatory feeding behaviors were classified as bioirrigators (Herringshaw et al., 2017; Kristensen et al., 2012). Small plug-shaped burrows such as *Conichnus* and *Bergaueria* are common representatives of bioirrigators in the Ediacaran and Terreneuvian, as well as larger, typically deeper U- and J-shaped trace fossils such as *Arenicolites* and *Diplocraterion* which are more common in the Terreneuvian (Table 1). Trace fossils such as *Treptichnus* and *Streptichnus*, which are vertically oriented and created in a conveying-type behavior and would have likely connected the sediment–water interface with the porewaters multiple

TABLE 1 Ediacaran and Terreneuvian ichnogenera and assigned bioturbation behavior (biomixing or bioirrigation) with data from Buatois et al. (2020).

Ediacaran		Terreneuvian	
Ichnogenera	**Behavior**	**Ichnogenera**	**Behavior**
Archaeonassa	Biomixing	*Alcyonidiopsis*	Biomixing
Arenicolites	Bioirrigation	*Allocotichnus*	Biomixing
Bergaueria	Bioirrigation	*Altichnus*	Bioirrigation
Circulichnus	Biomixing	*Archaeonassa*	Biomixing
Conichnus	Bioirrigation	*Arenicolites*	Bioirrigation
Gordia	Biomixing	*Asaphoidichnus*	Biomixing
Helminthoidichnites	Biomixing	*Astropolichnus*	Bioirrigation
Helminthopsis	Biomixing	*Bergaueria*	Bioirrigation
Lamonte	Biomixing	*Cheiichnus*	Biomixing
Multina	Biomixing	*Circulichnus*	Biomixing
Nenoxites	Biomixing	*Cochlichnus*	Biomixing
Palaeophycus	Biomixing	*Conichnus*	Bioirrigation
Parapsammichnites	Biomixing	*Cruziana*	Biomixing
Planolites	Biomixing	*Curvolithos*	Biomixing
Streptichnus	Bioirrigation	*Cylindrichnus*	Biomixing
Torrowangea	Biomixing	*Dactyloidites*	Biomixing
Treptichnus	Bioirrigation	*Dendrorhaphe*	Biomixing
		Diplocraterion	Bioirrigation
		Diplopodichnus	Biomixing
		Gordia	Biomixing
		Guanshanichnus	Biomixing
		Gyrolithes	Bioirrigation
		Heliochone	Biomixing
		Helminthoidichnites	Biomixing
		Helminthopsis	Biomixing
		Laevicyclus	Bioirrigation
		Lingulichnus	Bioirrigation
		Multina	Biomixing
		Oichnus	Bioirrigation
		Oldhamia	Biomixing
		Palaeophycus	Biomixing
		Paleodictyon	Biomixing
		Phycodes	Bioirrigation
		Pilichnus	Biomixing
		Planolites	Biomixing
		Protopaleodictyon	Biomixing
		Protovirgularia	Biomixing
		Psammichnites	Biomixing
		Rhizocorallium	Biomixing
		Rosselia	Bioirrigation
		Saerichnites	Biomixing
		Skolithos	Bioirrigation
		Syringomorpha	Bioirrigation

TABLE 1 (Continued)

Ediacaran		Terreneuvian	
Ichnogenera	Behavior	Ichnogenera	Behavior
		Taenidium	Biomixing
		Tasmanadia	Biomixing
		Teichichnus	Biomixing
		Thalassinoides	Bioirrigation
		Torrowangea	Biomixing
		Treptichnus	Bioirrigation
		Trichophcyus	Biomixing
		Trypanites	Bioirrigatoin
		Volkichnium	Biomixing
		Zoophycos	Biomixing

Note: Full dataset is available in Data S1.

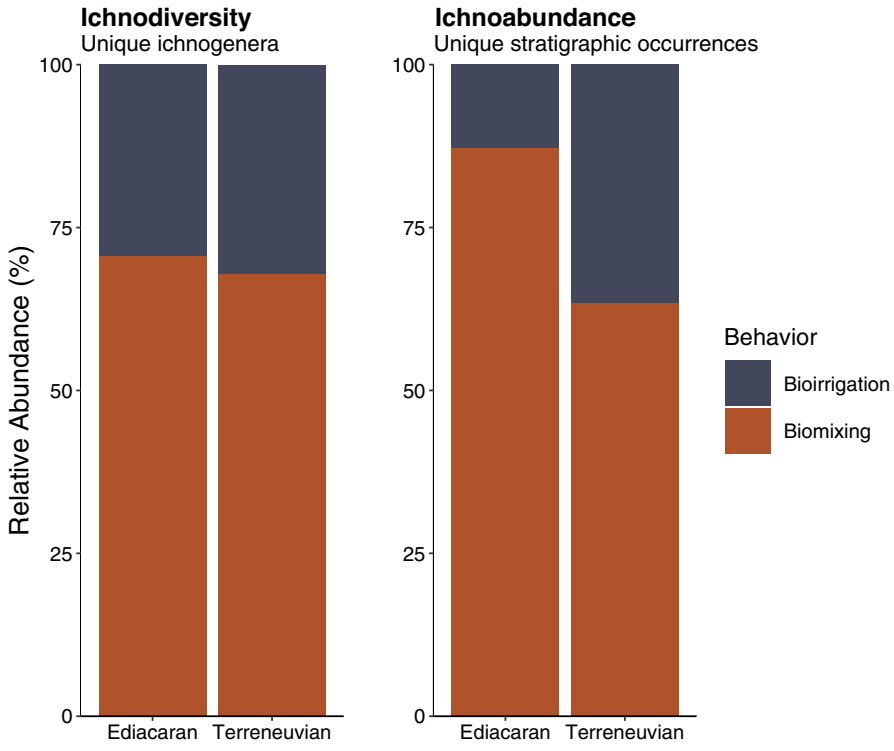

FIGURE 1 Biomixing and bioirrigation across the Ediacaran–Cambrian transition. Relative abundance of bioturbation behaviors based on ichnodiversity (number of unique ichnogenera in Table 1) and ichnoabundance (number of unique stratigraphic occurrences of ichnogenera in Table 1) for each time bin. Dark blue area of bar graphs indicates bioirrigation, and dark orange area indicates biomixing. Data are based on Buatois et al. 2020 and available in Data S1.

times throughout the burrow length, were also classified as bioirrigation trace fossils (Herringshaw et al., 2017; Table 1).

Ichnodiversity increases significantly in the Terreneuvian (Table 1). In the Ediacaran, 17 ichnogenera are present, versus 53 ichnogenera in the Terreneuvian (Table 1; Data S1; Buatois et al., 2020). However, there is only a small change in the ratio of biomixing to bioirrigation ichnogenera. 70.5% ($n = 12$) of ichnogenera in the Ediacaran and 67.9% ($n = 36$) of ichnogenera in the Terreneuvian are biomixers, and 29.5% ($n = 5$) of ichnogenera in the Ediacaran and 32.1% ($n = 17$) of ichnogenera in the Terreneuvian are bioirrigators (Figure 1). In contrast, from the unique stratigraphic occurrences (or ichnoabundance, where an ichnogenus occurrence is equal to each unique stratigraphic unit in which it occurs), there are 94 ichnogenera occurrences in the Ediacaran and 426 ichnogenera occurrences in the Terreneuvian (Data S1; Buatois et al., 2020). When measured this way, the proportion of biomixer to bioirrigator occurrences does observably change across the Ediacaran–Cambrian boundary. In the Ediacaran, 87.2% ($n = 82$) of ichnogenera occurrences represent biomixing and only 12.8% ($n = 12$) represent bioirrigation, in contrast to the Terreneuvian, where only 63.4% ($n = 270$) of ichnogenera occurrences are biomixers and 36.6% ($n = 156$) of ichnogenera occurrences represent bioirrigators.

Finally, we calculated a global average Ediacaran biodiffusion coefficient of $D_{B,0} = 0.1$ cm^2 year^{-1} and a Terreneuvian biodiffusion coefficient of $D_{B,0} = 0.98$ cm^2 year^{-1}. We note that the BI values taken from the literature (Mángano & Buatois, 2014) may be sensitive to

sedimentation rates, but the BI values were compiled from similar shallow marine paleoenvironments, and thus we would not expect sedimentation rates to be a major caveat of our biodiffusion coefficient parameterization. Assuming bioirrigation scales proportionately to modern values ($D_{B,0}$ = 10 cm^2 year^{-1}, α_0 = 365 year^{-1}; Solan et al., 2019; van de Velde & Meysman, 2016) as biodiffusion coefficients do, we estimate a bioirrigation coefficient of α_0 = 3.65 year^{-1} for the Ediacaran (1% of modern intensity) and α_0 = 35.8 year^{-1} (9.8% of modern intensity) for the Terreneuvian.

3.2 | Model results: sensitivity analyses of chosen biodiffusion and bioirrigation coefficients

No matter the level of organic matter flux or bottom-water oxygen concentrations, the OPD shallows as the biodiffusion coefficient increases. Within the range around the Ediacaran and Terreneuvian biodiffusion coefficients (0–1 cm^2 year^{-1}), the sensitivity of the OPD is dependent on bottom-water oxygen concentrations and the organic matter flux (Figure 2). For example, at the lowest organic matter flux of $CH_2O_{tot,F}$ = 150 μmol cm^{-2} year^{-1}, increasing the biodiffusion from 0 to 1 cm^2 year^{-1} shoals the OPD only by greater than 0.5 cm for [$O_{2,BW}$] = 0.14 mM and, most significantly, only greater than 1 cm for [$O_{2,BW}$] = 0.28 mM. At a higher organic matter flux of $CH_2O_{tot,F}$ = 300 μmol cm^{-2} year^{-1}, the OPD is only shallowed by greater than 0.5 cm at [$O_{2,BW}$] = 0.28 mM. Finally, at the highest, more modern-like organic matter flux of $CH_2O_{tot,F}$ = 700 μmol cm^{-2} year^{-1}, increasing the biodiffusion coefficient in the same range does not shallow the OPD significantly, even at the highest bottom-water oxygen concentrations. The OPD, therefore, is only significantly sensitive (shallowing > 1 cm) to small increases in low biodiffusion coefficients at very low organic matter fluxes and near modern bottom-water oxygen concentrations ([$O_{2,BW}$] = 0.28 mM), which are unlikely boundary conditions for the late Ediacaran or Terreneuvian (Krause et al., 2018). In the bottom-water oxygen concentration range of [$O_{2,BW}$] = 0.07–0.14 mM, however, the OPD is not particularly sensitive to small changes in biomixing intensity, especially in the range between and around Ediacaran and Terreneuvian biodiffusion coefficients (Figure 2).

Results are similar for the sensitivity of the OPD to increasing bioirrigation coefficients. Most broadly, increasing bioirrigation intensity deepens the OPD. However, the sensitivity of the OPD to increases in bioirrigation intensity decreases with increasing organic matter flux, decreasing bottom-water oxygen concentrations, and increasing biomixing intensity (Figure S2). For most combinations of organic matter flux, bottom-water oxygen concentration, and biodiffusion coefficient, there is an inflection point in which a small change in the bioirrigation coefficient shifts the OPD from a shallow and partially to a fully oxygenated model sediment column (Figure S2). The bioirrigation coefficient at which this inflection point occurs, however, becomes larger with increased organic matter input and lower bottom-water oxygen concentrations (Figure S2). For example, at an organic matter flux of $CH_2O_{tot,F}$ = 150 μmol cm^{-2} year^{-1}, the inflection point only occurs at bottom-water oxygen concentrations above [$O_{2,BW}$] = 0.07 mM with Ediacaran biodiffusion and only above [$O_{2,BW}$] = 0.14 mM with a Terreneuvian biodiffusion coefficient (Figure S2) Furthermore, the inflection point occurs at higher bioirrigation coefficients as bottom-water oxygen concentrations are decreased (Figure S2). As organic matter fluxes increase, higher bottom-water oxygen concentrations and bioirrigation coefficients are required to cause the inflection point (Figure S2). Thus, increasing the bioirrigation coefficient only results in significant (>1 cm) changes in the OPD at very high, near-modern bioirrigation intensities, very low organic matter fluxes, and/or very high, near-modern bottom-water oxygen concentrations.

In summary, small changes to the already low estimated biodiffusion and bioirrigation coefficients should not significantly change the OPD, given the most likely Ediacaran and Terreneuvian bottom-water oxygen concentrations and organic matter flux boundary conditions. Furthermore, the estimated Ediacaran and Terreneuvian bioirrigation coefficients consistently fall behind the inflection point for all boundary conditions (Figure S2), indicating that the OPD is relatively insensitive to changes in bioirrigation intensity within the range of our bioturbation parameters. Additionally, it is important to note that, although the estimated Ediacaran and Terreneuvian biodiffusion and bioirrigation coefficients may not precisely represent the reality of Ediacaran and Terreneuvian bioturbators, the insensitivity of the OPD at lower oxygen concentrations and around an organic matter flux of $CH_2O_{tot,F}$ = 300 μmol cm^{-2} year^{-1} (Tarhan et al., 2021) suggests that both time periods' estimated biodiffusion and bioirrigation coefficients are broadly accurate in predicting relative changes in the OPD through the Ediacaran–Cambrian transition.

3.3 | Model results: sensitivity analyses of the OPD to bioturbation intensities

The results of our sensitivity analyses underscore the similarity in magnitude of impact of Ediacaran and Terreneuvian bioturbation on the OPD and its sensitivity to environmental change, particularly in comparison to results for no bioturbation and modern bioturbation (Figure 3). At all organic matter fluxes, Ediacaran and Terreneuvian bioturbation have an insignificant impact on the depth of oxygen penetration into the sediment. At the lowest organic matter flux in our Ediacaran–Cambrian boundary conditions (150 μmol cm^{-2} year^{-2}), the OPD without bioturbation deepens by 0.68 cm when bottom-water oxygen concentrations are increased from the low to high range of Ediacaran–Cambrian boundary conditions (0.07–0.14 mM). In contrast, neither Ediacaran or Terreneuvian bioturbation impact the OPD significantly to magnitudes greater than 0.5 cm. As the organic matter flux increases, the impact of Ediacaran and Terreneuvian bioturbation is even less significant. In contrast, with modern bioturbation, the OPD is significantly deepened on the order of several centimeters when bottom-water oxygen concentrations are increased from 0.07 to 0.14 mM until the organic matter flux reaches around 400 μmol cm^{-2} year^{-1}. At very high organic

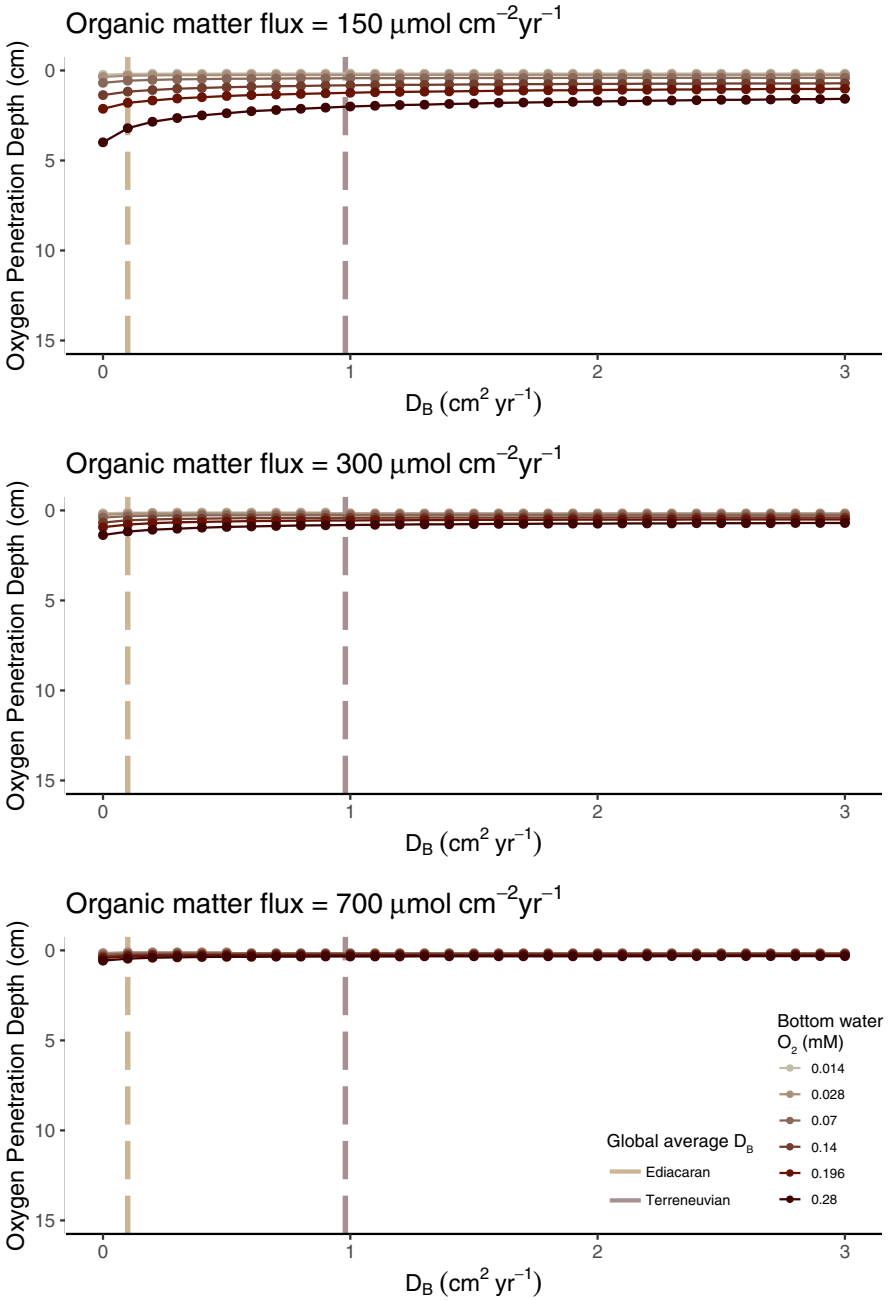

FIGURE 2 Sensitivity analyses of biodiffusion coefficients. Sensitivity analyses for chosen Ediacaran and Terreneuvian biodiffusion coefficients at increasing bottom-water oxygen concentrations and three different organic matter fluxes. Four dotted lines are the simulated OPD as the biodiffusion coefficient increases at four different bottom-water oxygen levels. Oxygen concentrations increase as colors scale from beige to dark red. The Ediacaran biodiffusion coefficient is 0.1 cm^2 year^{-1} and the Terreneuvian biodiffusion coefficient is 0.98 cm^2 year^{-1}, which are plotted as the brown and purple dashed lines, respectively. Bioirrigation coefficient here is 0 year^{-1}. Full boundary conditions are given in Table S6.

matter concentrations, increasing bottom-water oxygen concentrations within the low Ediacaran–Cambrian boundary conditions does not result in any major (>0.5 cm) change between no bioturbation, Ediacaran bioturbation, Terreneuvian bioturbation, or modern bioturbation.

Our results also underscore the differences in effects on the OPD between biomixing and bioirrigation (Figure 4). Holding either bottom-water oxygen concentrations or organic matter fluxes consistent, biomixing shallows the OPD, and bioirrigation deepens it. Moreover, increased biomixing decreases the sensitivity of the OPD to changes in bottom-water oxygen concentrations, while the opposite is true for bioirrigation. As biomixing intensity increases from Ediacaran to modern, the OPD becomes increasingly insensitive to changes in organic matter or bottom-water oxygen concentrations (Figure 4). Interestingly, the difference in the magnitude of the OPD deepening in the range of Ediacaran–Cambrian boundary condition bottom-water oxygen concentrations ($[O_{2,BW}]$ = 0.07–0.14 mM) between biomixing and bioirrigation in the Ediacaran and Terreneuvian is not significant, particularly at high organic matter fluxes (Figure 4). However, modern bioirrigation causes the OPD to be very significantly deepened, as the entire model sediment column in oxygenated (Figure 4). These trends are reflected by the increasing size of shallow OPD contour spaces as biomixing intensity increases versus the increasing size of the deep and >10 cm OPD contour spaces as bioirrigation intensity increases. However, it is important to note that these very deep simulated OPDs would not be found in modern environments, largely due to the anactualistic boundary

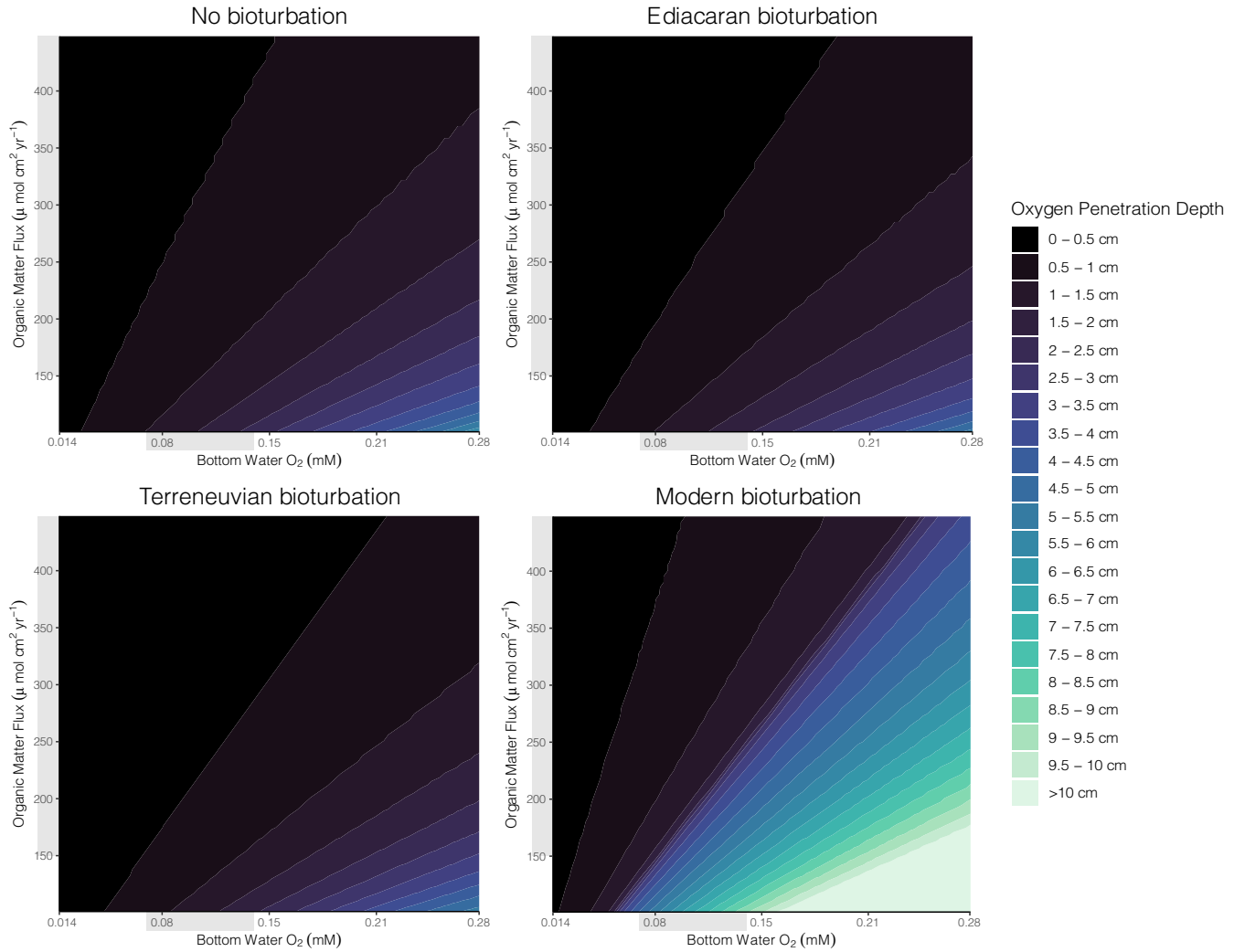

FIGURE 3 Contour plots of modeling results with no bioturbation and Ediacaran, Terreneuvian, and modern bioturbation parameters. Ediacaran bioturbation parameters are $D_{B,0} = 0.1$ cm^2 year^{-1} and $\alpha_0 = 3.65$ year^{-1}. Terreneuvian bioturbation parameters are $D_{B,0} = 0.98$ cm^2 year^{-1} and $\alpha_0 = 35.8$ year^{-1}. Modern bioturbation parameters are $D_{B,0} = 10$ cm^2 year^{-1} and $\alpha_0 = 365$ year^{-1}. Each colored contour indicates resulting simulated OPD depths at the same $x - x+0.5$ cm range. Colors are consistent across each plot and correspond to the legend on the right, where dark purple colors are shallowest OPDs, and light green colors are the deepest OPDs. Gray bars on axes are estimated ranges of organic matter flux and bottom-water oxygen concentrations, which are discussed in the text. Full boundary conditions are given in Table S7.

conditions of very high bottom-water oxygen concentrations and very low organic matter fluxes in shallow marine environments. In general, oxygen penetration depths measured from the inner to outer shelf (0–200 m water depth) do not reach 2.5 cm (Jørgensen et al., 2022). Modern environments with OPDs greater than 10 cm are limited to water depths greater than 2000 m, where bottom-water oxygen concentrations are high and net primary productivity is low (Jørgensen et al., 2022).

3.4 | Model results: impact of organic matter flux on the effect of bioturbation

Our results also demonstrate that organic matter flux would have exerted a major control on the magnitude of impact that Ediacaran-Cambrian transition bioturbation could have had on the OPD (Figure 5). At bottom-water oxygen concentrations of $[O_{2,BW}] = 0.07$ mM, increasing bioturbation intensity has an insignificant, sub-centimeter scale impact on the OPD, and increasing organic matter further mutes the impact of bioturbation. For example, at an organic matter flux of $CH_2O_{tot,F} = 150$ µmol cm^{-2} year^{-1}, the OPD is 0.66 cm with no bioturbation, shallows by less than centimeter with Ediacaran and Terreneuvian bioturbation and deepens by less than a centimeter with modern bioturbation (Figure 5). As the organic matter flux increases to 300 and 450 µmol cm^{-2} year^{-1}, the OPD still shallows with Ediacaran and Terreneuvian bioturbation and deepens with modern bioturbation, but the magnitudes of change become increasingly insignificant as organic matter flux increases (Figure 5). In sum, Ediacaran and Terreneuvian bioturbation always shallow the OPD, while modern bioturbation always deepens

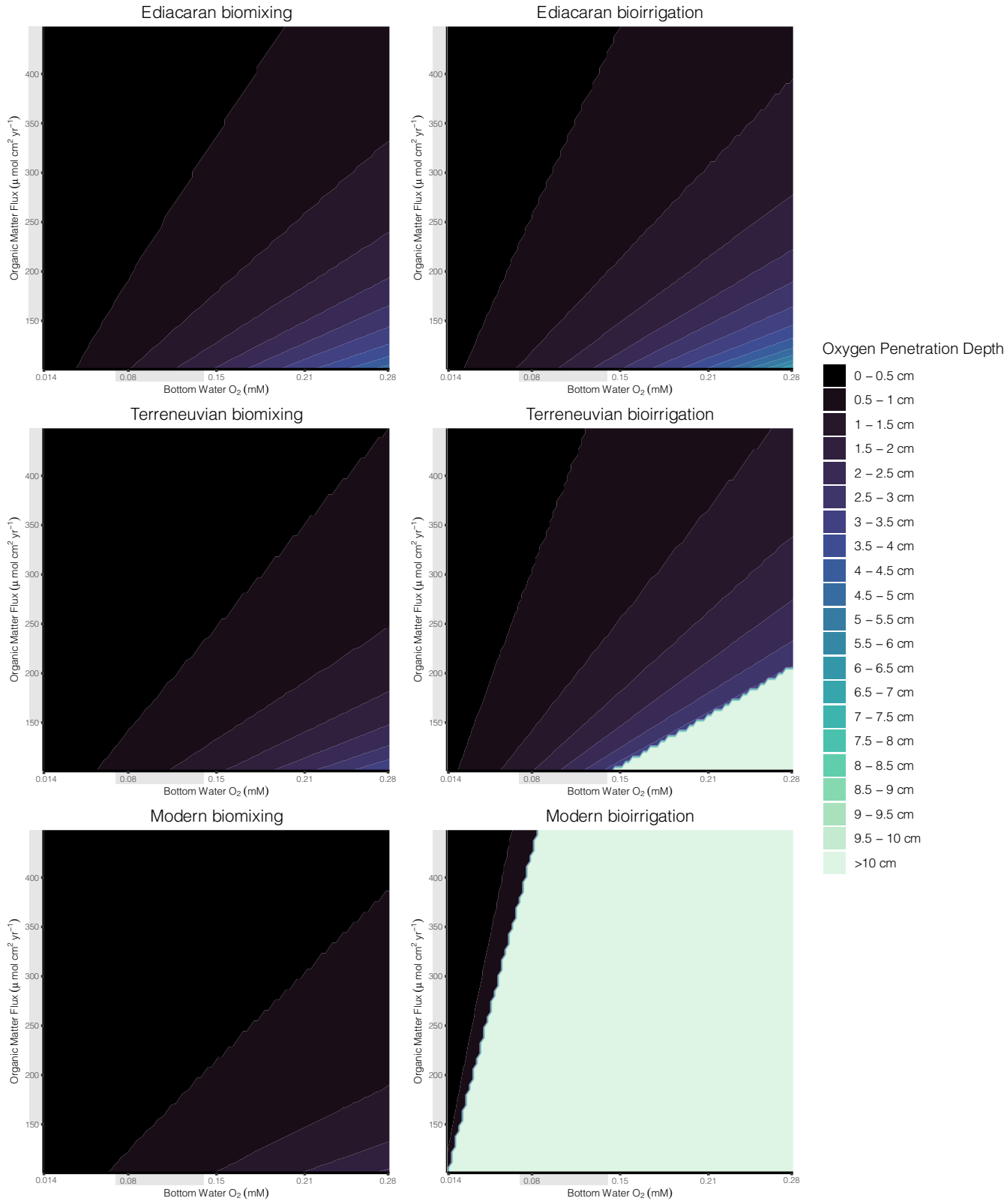

FIGURE 4 Contour plots of modeling results comparing biomixing versus bioirrigation at Ediacaran, Terreneuvian, and modern intensities. Biodiffusion coefficients are $D_{B,0} = 0.1$ cm^2 year^{-1} for Ediacaran biomixing, $D_{B,0} = 0.98$ cm^2 year^{-1} for Terreneuvian biomixing, and $D_{B,0} = 10$ cm^2 year^{-1} for modern biomixing. Bioirrigation coefficients are $\alpha_0 = 3.65$ year^{-1} for Ediacaran bioirrigation, $\alpha_0 = 35.8$ year^{-1} for Terreneuvian bioirrigation, and $\alpha_0 = 365$ year^{-1} for modern bioirrigation. For biomixing results, $\alpha_0 = 0$ year^{-1} for all three intensities. For bioirrigation results, $D_{B,0} = 0$ cm^2 year^{-1} for all three intensities. Color scale is consistent with Figure 3. Gray bars on axes are estimated ranges of organic matter flux and bottom-water oxygen concentrations, which are discussed in the text. Full boundary conditions are given in Table S7.

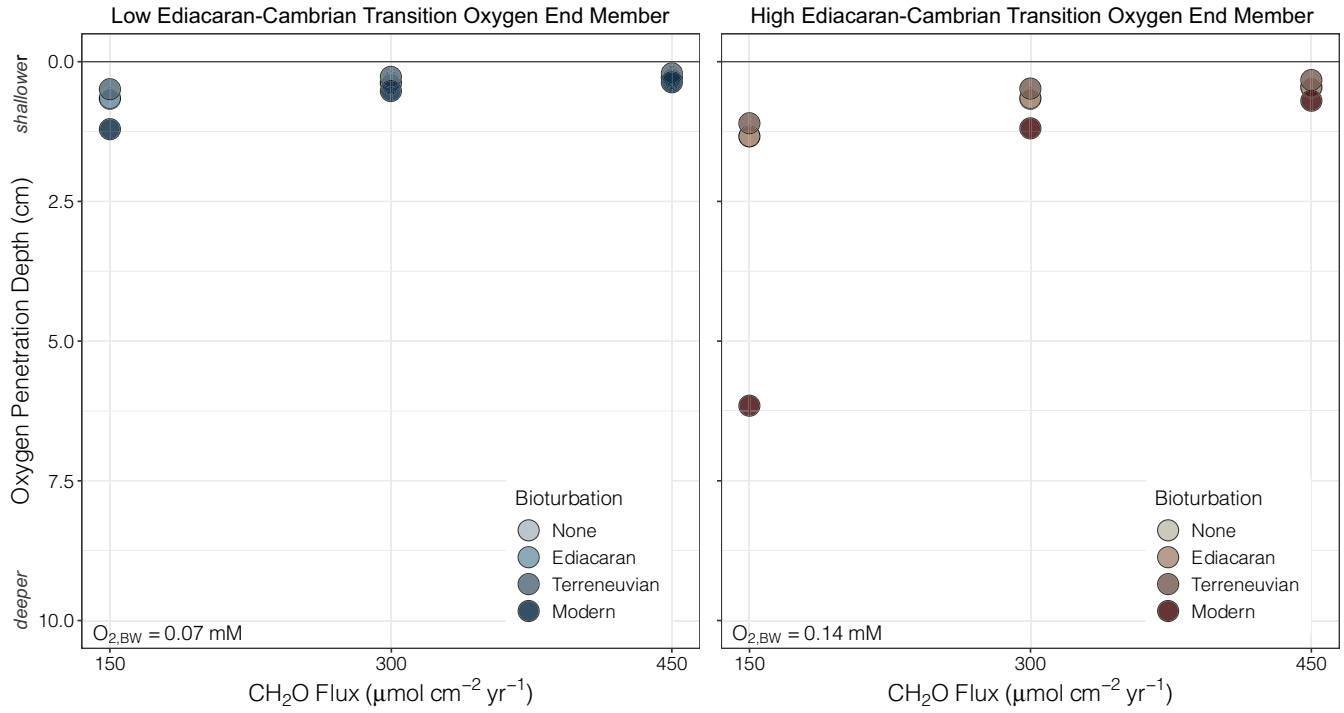

FIGURE 5 Effect of organic matter on OPD at different oxygen levels and bioturbation intensities. Simulation of the OPD at low (left, $[O_{2,BW}] = 0.07$ mM, 25% PAL) and high (right, $[O_{2,BW}] = 0.14$ mM, 50% PAL) end members for Ediacaran–Cambrian transition bottom-water oxygen concentrations at three different organic matter fluxes (500, 300, and 450 µmol cm^2 year^{-1}) and four intensities of bioturbation. See main text or Figure 3 for Ediacaran, Terreneuvian, and modern bioturbation parameters. Specific OPDs for each bioturbation intensity in all six scenarios given in the main text. Solid lines at 0 cm indicate the sediment–water interface. Full boundary conditions are given in Table S8.

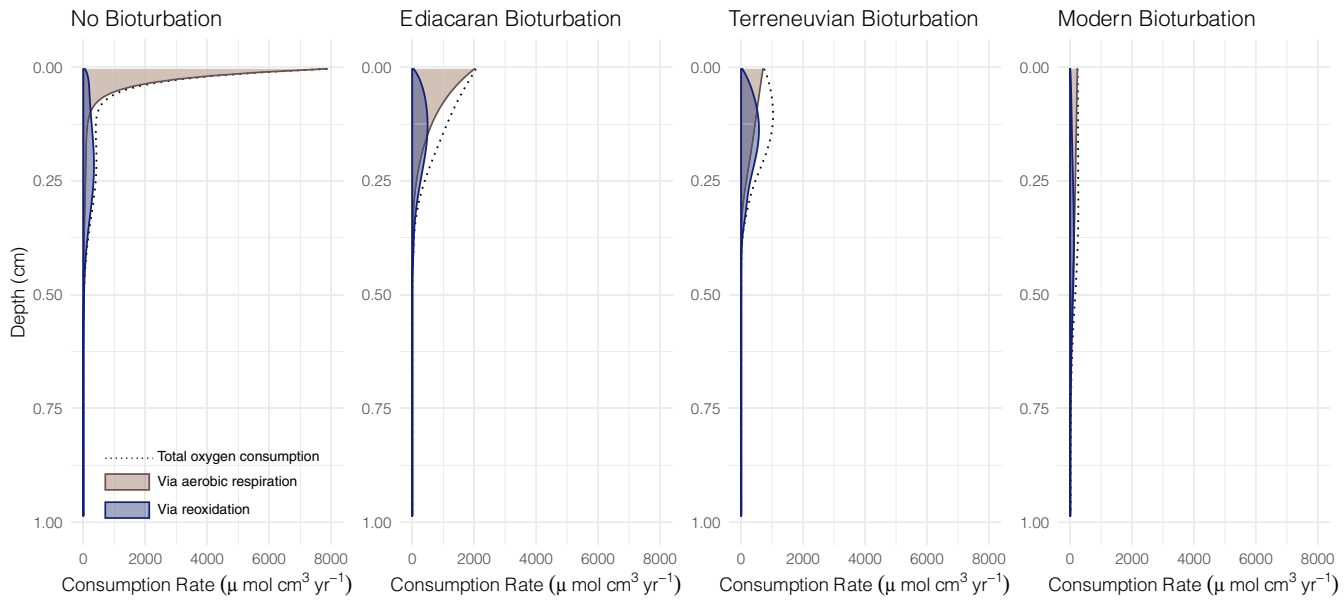

FIGURE 6 Oxygen consumption rate profiles in the upper 1 cm of the sediment column for no bioturbation and Ediacaran, Terreneuvian, and modern bioturbation parameters. Total oxygen consumption (dotted line) is broken up into aerobic respiration (red area) and reoxidation reactions (blue area). Ediacaran, Terreneuvian, and modern bioturbation parameters can be found in the main text or in Figure 3. Boundary conditions are listed in Table S9.

the OPD, but the significance of those changes decreases as the organic matter flux increases.

This pattern holds true but is even more pronounced when oxygen is increased to $[O_{2,BW}] = 0.14$ mM (Figure 5), such that more significant changes in the OPD can occur at higher bottom-water oxygen concentrations. At the lowest organic matter flux of $CH_2O_{tot,F}$ = 150 µmol cm^{-2} year^{-1}, the OPD is 1.3 cm with no bioturbation, does not change with Ediacaran bioturbation, shallows by

less than 1 cm with Terreneuvian bioturbation, and significantly deepens to 6.2 cm with modern bioturbation (Figure 4). When the organic matter flux is increased to $CH_2O_{tot,F}$ = 300 μmol cm^{-2} $year^{-1}$, the OPD shoals to 0.66 cm with no bioturbation, also shallows insignificantly with both Ediacaran and Terreneuvian bioturbation, and still deepens, although with a much smaller magnitude, to 1.2 cm with modern bioturbation (Figure 5). Finally, at the highest organic matter flux of $CH_2O_{tot,F}$ = 450 μmol cm^{-2} yea r^{-1}, the OPD is further shallowed to 0.46 cm with no bioturbation, shallows negligibly with both Ediacaran and Terreneuvian bioturbation, and only slightly deepens with modern bioturbation. Thus, only at very low organic matter fluxes and higher bottom-water oxygen concentrations within the range of Ediacaran–Cambrian boundary conditions is even modern bioturbation capable of significantly impacting the OPD on a magnitude of greater than 1 cm. These results are consistent when the same OPD simulations are conducted using a more geochemically complex model (Zhao et al., 2020), which results in sediment oxygen profiles that are consistently not significantly impacted by Ediacaran or Terreneuvian bioturbation (Figures S7 and S8).

3.5 | Model results: bioturbation intensities and oxygen consumption rates

Finally, we focus on the effects of biomixing versus bioirrigation and different intensities of bioturbation on oxygen consumption rates to investigate a mechanism for why different modes of bioturbation have such different impacts on the OPD. Different intensities of bioturbation alter the nature of oxygen consumption in the sediment. Without bioturbation, the rate of maximum oxygen consumption occurs at the sediment–water interface primarily via aerobic respiration. Oxygen consumption via reoxidation reactions consists of only a minor component of total aerobic respiration but does become the dominant pathway below around 0.11 cm when aerobic respiration decreases significantly (Figure 6). With Ediacaran bioturbation, the maximum rate of oxygen consumption decreases but still occurs at the sediment–water interface. Oxygen is still primarily consumed via aerobic respiration until around 0.15 cm, where reoxidation reactions become slightly dominant (Figure 6). With Terreneuvian bioturbation, the maximum oxygen consumption rate is further decreased and shifts away from the sediment–water interface to a sediment depth of 0.11 cm and, for the first time, oxygen is consumed primarily via reoxidation instead of aerobic respiration (Figure 6). Finally, with modern bioturbation, oxygen consumption rates are significantly decreased overall. The maximum oxygen consumption rate occurs at a sediment depth of 0.30 cm and is consumed primarily via aerobic respiration until around 0.5 cm, where oxygen consumption via reoxidation pathways becomes dominant (Figure 6).

Whether or not biomixing or bioirrigation is the dominant bioturbation behavior can also significantly change the fate of oxygen in the sediment. Increasing biomixing both shifts the maximum rate of oxygen consumption further below the sediment–water interface and increases the rate of oxygen consumption via reoxidation reactions (Figure S3). In contrast, increasing the intensity of bioirrigation does not change the depth nor dominant pathway of maximum oxygen consumption. For Ediacaran, Terreneuvian, and modern bioirrigation intensities, all three depths of maximum oxygen consumption are at the sediment–water interface and dominantly driven by aerobic respiration. Increasing bioirrigation does, however, most significantly decrease the total rate of oxygen consumption via reoxidation reactions, thereby also decreasing the total oxygen consumption occurring below the zone in which aerobic respiration dominates (Figure S3).

4 | DISCUSSION

4.1 | Geobiological implications for the Ediacaran–Cambrian transition trace fossil record

The trace fossil record of the Ediacaran and Terreneuvian suggests that, globally, biomixers were more common than bioirrigators during the Ediacaran–Cambrian transition. Ichnodiversity clearly increased (around three-fold) from the Ediacaran to the Terreneuvian (Table 1; Figure 1; Buatois et al., 2020; Buatois & Mángano, 2018; Mángano & Buatois, 2020). However, there was no change in the proportion of biomixers to bioirrigators in newly evolved behaviors (Figure 1). Whether the dominance of biomixing is measured in terms of unique ichnogenera or unique stratigraphic occurrences, biomixing was the dominant bioturbation behavior in the Ediacaran and remains so in the Terreneuvian. This recorded dominance of biomixing is perhaps surprising, given previous interpretations that the lack of a sedimentary mixed layer in the early Cambrian is representative of bioirrigation being the dominant bioturbation behavior (Tarhan, 2018a), although ultimately reflects the overall weak intensity of Ediacaran–Cambrian transition bioturbators.

Bioirrigation activity does appear to have increased from the Ediacaran to the Terreneuvian based on ichnoabundance from unique stratigraphic occurrences (Figure 1). This could reflect a variety of factors, ranging from facies bias to an environmentally driven increase in bioirrigators' activity or population densities. First, this could reflect a paleoenvironmental bias, as early bioirrigators may have been restricted to certain nearshore paleoenvironments (Seilacher, 1967) that might be more represented in the Terreneuvian trace fossil record. Alternatively, bioirrigators may have become more frequently preserved in the trace fossil record if biomixing intensity decreased, as strong sediment disruption can erase sessile animals' trace fossils from the mixed layer (Tarhan, 2018b) and strong deposit feeder biomixing activity can exclude bioirrigating suspension feeders from ecosystems (Rhoads & Young, 1970). However, the lack of a globally widespread, well-developed mixed layer in shallow marine environments (Tarhan, 2018a; Tarhan et al., 2015) and the dominance of biomixers over bioirrigators in the Ediacaran (Figure 1) suggest that the increase in bioirrigation trace fossil occurrences is not a taphonomic artifact. The most feasible explanation for these patterns is that bioirrigators became more active in the Terreneuvian, likely due to biotic innovations and changing global environmental conditions.

In particular, suspension feeders – which are generally effective bioirrigators – tend to be excluded from low-oxygen environments compared to deposit feeding biomixers (Rhoads, 1975), so an increase in bottom-water oxygen concentrations in global shallow marine environments would likely have allowed for the more bioirrigation trace fossil occurrences in the fossil record. Suspension feeders also thrive in environments with high amounts of suspended organic detritus (Rhoads, 1975), so an increase in their trace fossil abundances through the Ediacaran–Cambrian transition may also reflect changes in the organic matter cycle which increased their food availability (Sperling & Stockey, 2018).

Not all biomixing and bioirrigating fauna would be expected to have the same environmental impact as each other. This is especially important in considering any local effects that some rare, particularly large and architecturally complex ichnogenera in the Ediacaran and Terreneuvian may have. The ecosystem engineering impacts (modification of resource availability (Jones et al., 1994)) of specific ichnogenera have been previously explored in the Fortunian, and it was concluded that trace fossils such as *Thalassinoides*, *Treptichnus*, *Teichichnus*, and *Gyrolithes* represent relatively high-impact bioturbation behaviors with a more significant capability to alter the benthic environment for other animals than other contemporary ichnogenera (Herringshaw et al., 2017). As these four ichnogenera are bioirrigation trace fossils, our results support the notion that the animals that made those trace fossils would have been well-suited for oxygenating the sediments around them. In the Ediacaran, *Parapsammichnites* and *Arenicolites* likely represent the major bioturbators most significant for impacting oxygen in the sediment (Table 1). *Parapsammichnites*, which provides the earliest evidence of sediment bulldozing (relatively large deposit feeding behaviors that displace significant amounts of sediment; Buatois et al., 2018; Darroch et al., 2020), represents the biomixing behavior most likely to have had the strongest impact. *Parapsammichnites* is the largest biomixing trace fossil in the Ediacaran, as it is the first centimeter-scale coelomic-grade trace fossil that appears in the rock record (Buatois et al., 2018), and thus likely resulted in the largest amount of organic matter mixing throughout the sediment to stimulate oxygen consumption and ultimately shallowed the OPD. However, we do note that *Parapsammichnites* does not have a major vertical component. Densely bioturbated bedding planes covered in small trace fossils such as *Helminthoidichnites* and *Helminthopsis* (Darroch et al., 2020) may also represent collectively strong biomixing by many bioturbators. However, modern research suggests that biomixing rates are more impacted by animal size than density (Sandnes et al., 2000). Thus, *Parapsammichnites* remains the best representation of early intense biomixing. However, *Parapsammichnites* is rare in the Ediacaran and currently only identified in one stratigraphic unit in the Nama Group, Namibia (Buatois et al., 2018; Darroch et al., 2020), and thus, it is unlikely to represent a global forcing for changes in benthic oxygen cycling. Among Ediacaran bioirrigators, *Arenicolites* is the best evidence for the presence of macrofauna that could have significantly oxygenated the sediment, as the trace-maker would have likely ventilated its U- and J-shaped burrows down to a few centimeters (Oji et al., 2018). However, like *Parapsammichnites*, *Arenicolites* is exceptionally rare in the Ediacaran, and in isolation may have not had a large enough effect to significantly increase sediment oxygen concentrations, as oxygen diffusion away from the burrow in the sediment would be quickly consumed by biogeochemical reactions (Aller, 1980). More common terminal Ediacaran bioirrigation trace fossils such as *Treptichnus* and *Streptichnus*, which have been previously interpreted as high-ecosystem engineering impact Ediacaran trace fossils (Cribb et al., 2019), likely also represent relatively intense Ediacaran bioirrigation, although their small size prior to the Ediacaran–Cambrian boundary (Darroch et al., 2020) suggests their effects were likely quite limited.

Finally, not every benthic ecosystem in the Ediacaran and Terreneuvian would be expected to have the same composition of biomixers and bioirrigators, nor the same biological activity. For example, from an ichnofacies perspective, bioirrigators would likely have been more common in nearshore environments with abundant wave-suspended organic matter, whereas biomixers would likely have been more common in deeper offshore areas where organic matter was more significantly deposited at the seafloor (Rhoads, 1975; Seilacher, 1967). However, we note that for the Ediacaran in particular, biomixers may have been more dominant in nearshore environments where microbial mats were abundant and could serve as a food source for deposit feeders. Similarly, regional-scale palaeoceanographic and environmental differences would have certainly influenced the distribution of bioturbation intensity at any given time. In the modern ocean, bioturbation intensity and benthic community structure are often controlled by ecophysiological factors such as food (e.g., organic matter flux), bottom-water oxygen concentrations, and temperature at the sea floor (Levin et al., 2001; Smith & Rabouille, 2002; Woolley et al., 2016). These ecophysiological factors are certainly not homogenous throughout the ocean today, and thus are not expected to have been equal in every paleoenvironment throughout Earth history.

4.2 | Impact of Ediacaran–Cambrian bioturbation on sedimentary oxygen dynamics

These modeling results ultimately offer little support to the hypothesis that early bioturbators could have significantly oxygenated the sediment column. When biomixing and bioirrigation are considered separately, our results show that as biomixing intensity increases from Ediacaran to modern, the OPD shoals significantly, and in contrast, increasing bioirrigation intensity from Ediacaran to modern intensities deepens the OPD (Figure 4). This is a key result, considering the dominance of biomixing in the Ediacaran and Terreneuvian fossil records (Figure 1). Furthermore, and most critically, our modeling results ultimately indicate that Ediacaran and Terreneuvian bioturbation had an insignificant impact on the OPD, even slightly shoaling the OPD. Although bioirrigation trace fossil occurrences do increase in the Terreneuvian (Figure 1), it is important to note that for bioirrigation alone there is a negligible OPD-deepening effect within the

plausible lower range of Ediacaran and Terreneuvian bottom-water oxygen concentrations ($[O_{2,BW}]$ = 0.07–0.14 mM) and organic matter fluxes ($CH_2O_{tot,F}$ = 150–450 μmol cm^{-2} $year^{-1}$; Figures 4 and 5). Overall, given the context from the trace fossil record that biomixers were more dominant than bioirrigators (Table 1; Figure 1) and geochemical evidence that bottom-water oxygen concentrations and organic matter fluxes were lower than in modern environments (Fakhraee et al., 2020; Krause et al., 2018; Lu et al., 2018; Spering et al., 2021; Sperling & Stockey, 2018), we take these modeling results as evidence that neither Ediacaran nor Terreneuvian bioturbators were capable of significantly oxygenating the sediment column. Thus, Ediacaran–Cambrian transition bioturbators were unlikely to have promoted habitability of deeper sediment layers for other aerobic infauna (c.f. Mángano & Buatois, 2017), nor were they likely capable of causing such significant changes to the redox structure of the seafloor that it resulted in altered biogeochemical cycles that influenced atmospheric oxygen concentrations (c.f. Dahl et al., 2019).

Previous work has argued that local well-developed mixed layer depths in the Terreneuvian would increase oxygen concentrations by removing microbial mats to promote oxygen diffusion into the sediment (Gougeon et al., 2018). However, sediment mixing is not equivalent to sediment oxygenation. A well-developed mixed layer would result from strong biomixing, not bioirrigation (Boudreau, 1998; Tarhan, 2018a), and our results suggest that such an increase in biomixing intensity would result in a shallowing of the OPD (Figure 4). Globally, the mixed layer depth does not appear to have been well developed until later in the Paleozoic (Tarhan et al., 2015). We do find that the mixed layer depth deepens – and thereby biomixing intensity increases – slightly in the Terreneuvian (Table S10), but our results ultimately suggest that such a level of increase in bioturbation intensity from the Ediacaran to the Terreneuvian had a negligible impact on the OPD (Figure 3). Previous work has also argued that the evolution of early complex bioturbation ecosystem engineering behaviors may have driven significant biogeochemical change in the Ediacaran (Cribb et al., 2019). Although complex trace fossils that represent relatively impactful ecosystem engineering behaviors increase in intensity in the terminal Ediacaran (Cribb et al., 2019) and into the Fortunian (Herringshaw et al., 2017), not all high-impact benthic ecosystem engineering causes sediment oxygenation, and it was unlikely that such change resulted in any large-scale sediment oxygenation event.

These results all suggest a more protracted evolution and ecological impact of bioturbation as major global ecosystem engineers that significantly change resourace availability in shallow marine environments until later in the Paleozoic (Tarhan et al., 2015), at least for benthic oxygen dynamics. However, early bioturbators may have had impacts on other critical biogeochemical cycles during this interval, including phosphorus, organic carbon, and sulfur (Boyle et al., 2014; Canfield & Farquhar, 2009; Tarhan et al., 2021; van de Velde et al., 2018), which are critical for the evolution of marine ecosystems but not studied here. For example, we do find that increasing bioturbation intensity changes the burial of organic matter and organic matter and FeS, although the magnitude of that change is a factor of organic matter delivery to the seafloor and bottom-water oxygen concentrations (Figure S5). Additionally, the subset of simulations we conducted using the more geochemically complex model from Zhao et al. (2020) does not consistently result in the same OPD shoaling (Figures S7 and S8), underscoring the potential importance of the complex, non-linear impacts that bioturbation has on biogeochemical cycles like iron and phosphorus (van de Velde et al., 2020). Future work investigating the role that early bioturbators played in other biogeochemical cycles that exerted major controls on benthic ecology will be critical for mechanistically linking the radiations observed in both the trace fossil and body fossil records in the Cambrian and Early Paleozoic.

Our modeled oxygen consumption profiles help mechanistically explain why biomixing and bioirrigation, as well as the different bioturbation intensities, have such different impacts on the OPD. The primary effect of increasing biomixing intensity on oxygen consumption is shifting the maximum zone of oxygen consumption downwards and increasing oxygen consumption via reoxidation (Figure S3). This occurs because biomixing transports more organic matter downwards below the oxic–anoxic interface to stimulate anaerobic remineralization pathways, which then results in the increased production of reduced compounds that consume oxygen via reoxidation reactions near the oxic–anoxic interface (Figure S3). Furthermore, as long as sediments are supplied enough organic matter for oxygen consumption to occur, biomixing will shift the zone of maximum oxygen consumption away from the sediment–water interface, thus making it more difficult for oxygen to diffuse into the sediment to resupply what is lost to consumption (van de Velde & Meysman, 2016). In contrast, the primary effect of increasing bioirrigation intensity is the injection of oxygen into the deeper sediment column coupled with decreased oxygen consumption via reoxidation, which is due to reduced compounds produced by anaerobic respiration being flushed out of the sediment column by bioirrigation (Aller & Aller, 1998; van de Velde & Meysman, 2016). Additionally, bioirrigation (as it is formulated here) does not transport organic matter in the sediment, so it does not stimulate anaerobic respiration the same way biomixing does (van de Velde & Meysman, 2016). This maintains an oxygen consumption profile where oxygen is primarily consumed by aerobic respiration near the sediment–water interface (Berner & Westrich, 1985; Figure S3), in which oxygen can resupply itself via diffusion or, more significantly, via bioirrigation to greater sediment depths. When biomixing and bioirrigation are modeled together at different intensities, results show that Ediacaran and Terreneuvian bioturbation more closely resemble the effects of biomixing, where oxygen consumption via reoxidation reactions is stimulated, and for Terreneuvian bioturbation, the zone of maximum oxygen consumption is shifted downwards (Figure 6). This suggests that bioturbation-driven sediment oxygenation during the early Paleozoic was delayed until the effects of bioirrigation were, at some threshold, stronger than those of biomixing, resulting in a stronger supply of oxygen downwards to resupply consumed oxygen.

Strong, modern-like bioturbation can deepen the OPD, even at relatively low-oxygen and higher organic matter fluxes (Figures 3 and 5), demonstrating that bioturbators did, at some point in time,

evolve the capability of extensively oxygenating shallow marine sediments. Further work is needed to constrain when modern-like bioturbation evolved, but it was likely not until later in the Paleozoic or even Mesozoic (Tarhan et al., 2015). Rare occurrences of large, deep trace fossils that were likely more strongly bioirrigated do occur in the early Paleozoic (Zhang et al., 2017), but evidence for intense sediment churning and large three-dimensional network burrows is still uncommon globally even in late Ordovician trace fossils (Tarhan, 2018a; Tarhan et al., 2015). The increase in trace fossil size and density in late Silurian trace fossil assemblages, particularly among sediment bulldozers, may be the earliest evidence for strong biomixing (Tarhan et al., 2015). However, strong biomixing and bioirrigation behaviors are not commonly represented in the trace fossil record until the Mesozoic Marine Revolution, which promoted the rise of the Modern evolutionary fauna (Sepkoski, 1981), including more modern-like bioturbating infaunal communities with stronger intensities (Buatois & Mángano, 2018; Tackett & Bottjer, 2012). For example, trace fossils made by irregular echinoids first appear in the Mesozoic, and trace fossils created by crustaceans, bivalves, and worms become increasingly abundant after the Paleozoic (Buatois & Mángano, 2018). These deep network burrows that became more common in the Mesozoic are likely representative of the first major radiation of strong bioirrigators and burrow ventilators that were capable of significantly deepening the OPD and extensively oxygenating the sediments in their ecosystems.

4.3 | Potential environmental controls on benthic oxygen dynamics

Organic matter has a competing role in the potential for bioturbation-driven sediment oxygenation, as the magnitude of each intensity of bioturbation's effect is increasingly muted with increasing organic matter flux (Figure 5). Even at relatively high bottom-water oxygen concentrations, increasing the organic matter flux to the seafloor mutes the oxygenating impact even of modern bioturbation intensities (Figure 5). Thus, one might expect that relatively strong bioirrigators in well-oxygenated benthic environments may have been able to deepen the OPD, at least slightly, during the Ediacaran–Cambrian transition. However, long-term changes in the organic carbon cycle – such as the efficiency of organic carbon export and rapid delivery to the sediment surface – may have significantly increased carbon export efficiency at low atmospheric oxygen concentrations due to faster sinking fecal pellets or changes in ocean temperature (Boscolo-Galazzo et al., 2021; Fakhraee et al., 2020; Lu et al., 2018). Such an increase in organic matter flux to the seafloor would likely have muted any oxygenating effect of bioirrigators in the earliest Cambrian. Additionally, because more organic matter availability likely physiologically fueled biomixing deposit feeders (Sperling & Stockey, 2018), an increase in organic matter may have caused a shallowing of the OPD by both stimulating aerobic respiration and by increasing biomixing intensity that promotes oxygen consumption via reoxidation.

Finally, bioturbation can impact sediment oxygen dynamics in ways that have not been explicitly tested here. First, we note that bioturbation may impact the flux of oxygen into the sediment by influencing the benthic boundary layer, either by creating burrow structures that change sediment topography near the sediment–water interface or by changing the roughness of the sediment–water interface due to changing the size or distribution of microbial mats on the seafloor. This impact of bioturbation is likely only important on a very local scale, but nonetheless it is an important avenue for future research on the role of bioturbation in local-scale benthic ecology. Additionally, further work is needed to constrain how early bioturbators' disruption of microbial mats alone impacted sediment oxygenation. The hypothesis that the disappearance of microbial mats in the early Cambrian allowed for the diffusion of oxygen into sediment porewaters (Seilacher, 1999) has not been explicitly biogeochemically tested in terms of the impact of the ecological structure and metabolic diversity of microbial mat communities, nor has it been tested in terms of the fate of the organic matter in the microbial mat as it is bioturbated. In terms of the former, microbial mats dominated by photosynthetic cyanobacteria, which would be feasible for the very shallow marine settings that early bioturbators occupied, can actually increase oxygen concentrations in the porewaters relative to the water column (Gingras et al., 2011). Thus, depending on the physiology of the microbial communities, bioturbation and mining of microbial mats may have temporarily decreased sediment porewater oxygen concentrations. In terms of the latter, any downwards mixing of organic matter derived from microbial mats may have amplified the shallowing effect on the OPD, although the magnitude and duration of such an effect would depend on the reactivity of the organic matter being supplied to the sediment and within the microbial mat. We note that there may also be some specific macrofauna-microbial mat interactions that uniquely alter sediment oxygen cycling due to the nature of the microbial mat, but such interactions are difficult to constrain from the trace fossil record alone. Additionally, the importance of the role of microbial mats as a supply of organic matter depends on the prevalence of the mats in Ediacaran and Terreneuvian bioturbated stratigraphic units, which may be influenced by both real changes in abundance of microbial mats across the Ediacaran–Cambrian transition and the number of stratigraphic units which were deposited in the photic zone. However, our results suggest that, in general, increased biomixing of organic matter from the microbial mat downwards into the sediment would most likely promote a shallowing of the OPD regardless of any increased diffusive oxygen exchange between the sediment porewater and the overlying water column.

5 | CONCLUSIONS

In conclusion, the results of this study highlight three main findings. First, the trace fossil record of the Ediacaran and Terreneuvian suggests that bioturbators during the Ediacaran–Cambrian transition

were predominantly biomixers, not bioirrigators. Second, bioturbators during the Ediacaran–Cambrian transition were most likely not capable of significantly increasing oxygen concentrations in the shallow to deep sediment tiers, particularly given the dominance of biomixers in the trace fossil record. Third, the magnitude of bioturbation's oxygenating effect is regulated by organic matter dynamics, which may be particularly important as increased organic matter fluxes to the seafloor later in the Paleozoic (Fakhraee et al., 2020) may have fueled biomixers (Sperling & Stockey, 2018) while muting the oxygenating effect of later-evolved more intense bioirrigators. Further work is needed to constrain the role and nature of the disappearance of microbial mats in the early Cambrian, as well as Ediacaran and Terreneuvian biomixers' and bioirrigators' impacts on other key biogeochemical cycles, in order to better understand bioturbation's ecosystem engineering role in shaping benthic ecology in the early Paleozoic. However, our results ultimately suggest that the effects on the fate of oxygen in the sediment proposed by the Agronomic Revolution (Seilacher & Pflüger, 1994) were delayed until after the Ediacaran and Terreneuvian when a unique, optimal combination of organic matter dynamics, bottom-water oxygen concentrations, and biotic innovations allowed bioturbators to extensively oxygenate their sedimentary environments.

ACKNOWLEDGMENTS

The authors thank the anonymous reviewers who provided thorough and valuable feedback which have contributed to a much-improved manuscript. A.T.C. acknowledges support for this research which was provided by NSF-DEB 2051255. This is E6 (Ecological and Evolutionary Effects of Extinction and Ecosystem Engineers RCN) publication #1. Finally, we are grateful to Simon Darroch and Richard Stockey for their helpful insights and discussions.

CONFLICT OF INTEREST STATEMENT

The authors declare that they have no competing interests.

DATA AVAILABILITY STATEMENT

The version of the dataset adapted from Buatois et al. (2020) is available as part of the Supporting Information (Data S1). All model code used is available on Github (https://github.com/atcribb/Ediacaran-Cambrian-OPD-Controls) and Zenodo (10.5281/zenodo.6129454).

ORCID

Alison T. Cribb https://orcid.org/0000-0002-8604-6100
Sebastiaan J. van de Velde https://orcid.org/0000-0001-9999-5586

REFERENCES

Aller, R. C. (1980). Quantifying solute distributions in the bioturbated zone of marine sediments by defining an average microenvironment. *Geochimica et Cosmochimica Acta*, *44*, 1955–1965.

Aller, R. C. (1982). The effects of macrobenthos on chemical properties of marine sediment and overlying water. *Animal-Sediment Relations*, 53–102. https://doi.org/10.1007/978-1-4757-1317-6_2

Aller, R. C., & Aller, J. Y. (1998). The effect of biogenic irrigation intensity and solute exchange of diagenetic reaction rates in marine sediments. *Journal of Marine Research*, *56*, 905–936.

Berner, R. A., & Westrich, J. T. (1985). Bioturbation and the early diagenesis of carbon and sulfur. *American Journal of Science*, *285*, 193–206.

Boscolo-Galazzo, F., Crichton, K. A., Ridgwell, A., Mawbey, E. M., Wade, B. S., & Pearson, P. N. (2021). Temperature controls carbon cycling and biological evolution in the ocean twilight zone. *Science (New York, N.Y.)*, *371*, 1148–1152.

Boudreau, B. P. (1984). On the equivalence of nonlocal and radial-diffusion models for porewater irrigation. *Journal of Marine Research*, *42*, 731–735.

Boudreau, B. P. (1996). The diffusive tortuosity of fine-grained unlithified sediments. *Geochimica et Cosmochimica Acta*, *60*, 3139–3142.

Boudreau, B. P. (1997). *Diagenetic models and their implementation: Modelling transport and reactions in aquatic sediments*. Springer.

Boudreau, B. P. (1998). Mean mixed depth of sediments: The wherefore and the why. *Limnology and Oceanography*, *43*, 542–526.

Boyle, R. A., Dahl, T. W., Dale, A. W., Shields-Zhou, G. A., Zhu, M., Brasier, M. D., Canfield, D. E., & Lenton, T. M. (2014). Stabilization of the coupled oxygen and phosphorus cycles by the evolution of bioturbation. *Nature Geoscience*, *7*, 671–676.

Buatois, L. A., Almond, J., Mángano, M. G., Jensen, S., & Germs, G. J. B. (2018). Sediment disturbance by Ediacaran bulldozers and the roots of the Cambrian explosion. *Scientific Reports*, *8*, 4514.

Buatois, L. A., & Mángano, M. G. (2018). The other biodiversity record: Innovations in animal-substrate interactions through geologic time. *GSA Today*, *28*, 4–10.

Buatois, L. A., Mángano, M. G., Minter, N. J., Zhou, K., Wisshak, M., Wilson, M. A., & Olea, R. A. (2020). Quantifying ecospace utilization and ecosystem engineering during the early phanerozoic—The role of bioturbation and bioerosion. *Science Advances*, *6*, eabb0618.

Cai, W. J., & Sayles, F. L. (1996). Oxygen penetration depths and fluxes in marine sediments. *Marine Chemistry*, *52*, 123–131.

Canfield, D. E., & Farquhar, J. (2009). Animal evolution, bioturbation, and the sulfate concentration of the oceans. *Proceedings of the National Academy of Sciences of the United States of America*, *106*, 8123–8127.

Corsetti, F. A., & Hagadorn, J. W. (2000). Precambrian-Cambrian transition: Death Valley, United States. *Geology*, *28*, 299–302.

Cribb, A. T., Kenchington, C. G., Koester, B., Gibson, B. M., Boag, T. H., Racicot, R. A., Mocke, H., Laflamme, M., & Darroch, S. A. F. (2019). Increase in metazoan ecosystem engineering prior to the Ediacaran–Cambrian boundary in the Nama group, Namibia. *Royal Society Open Science*, *6*, 190548.

Dahl, T. W., Connelly, J. N., Li, D., Kouchinsky, A., Gill, B. C., Porter, S., Maloof, A. C., & Bizzarro, M. (2019). Atmosphere-ocean oxygen and productivity dynamics during early animal radiations. *Proceedings of the National Academy of Sciences of the United States of America*, *116*, 19352–19361.

Dale, A. W., Nickelsen, L., Scholz, F., Hensen, C., Oschlies, A., & Wallmann, K. (2015). A revised global estimate of dissolved iron fluxes from marine sediments. *Global Biogeochemical Cycles*, *29*(5), 691–707. https://doi.org/10.1002/2014gb005017

Darroch, S. A. F., Cribb, A. T., Buatois, L. A., Germs, G. J. B., Kenchington, C. G., Smith, E. F., Mocke, H., Neil, G. R. O., Schiffbauer, J. D., Maloney, K. M., Racicot, R. A., Turk, K. A., Gibson, B. M., Almond, J., Koester, B., Boag, T. H., Tweedt, S. M., & Laflamme, M. (2020). The trace fossil record of the Nama group, Namibia: Exploring the terminal Ediacaran roots of the Cambrian explosion. *Earth-Science Reviews*, *212*, 103435.

Droser, M. L., & Bottjer, D. J. (1986). A semiquantitative field classification of ichnofabric. *Journal of Sedimentary Research*, *56*, 558–559.

Dunne, J. P., Sarmiento, J. L., & Gnanadesikan, A. (2007). A synthesis of global particle export from the surface ocean and cycling through the ocean interior and on the seafloor. *Global Biogeochemical Cycles*, *21*, GB4006.

Emerson, S., Jahnke, R., & Heggie, D. (1984). Sediment-water exchange in shallow water estuarine sediments. *Journal of Marine Research*, *42*(3), 709–730. https://doi.org/10.1357/002224084788505942

Fakhraee, M., Planavsky, N. J., & Reinhard, C. T. (2020). The role of environmental factors in the long-term evolution of the marine biological pump. *Nature Geoscience*, *13*, 812–816.

Fick, A. (1855). Ueber diffusion. *Annalen der Physik*, *94*, 59–86.

Gingras, M., Hagadorn, J. W., Seilacher, A., Lalonde, S. V., Pecoits, E., Petrash, D., & Konhauser, K. O. (2011). Possible evolution of mobile animals in association with microbial mats. *Nature Geoscience*, *4*, 372–375.

Gougeon, R. C., Mángano, M. G., Buatois, L. A., Narbonne, G. M., & Laing, B. A. (2018). Early Cambrian origin of the shelf sediment mixed layer. *Nature Communications*, *9*, 1909.

Herringshaw, L. G., Callow, R. H. T., & McIlroy, D. (2017). Engineering the Cambrian explosion: The earliest bioturbators as ecosystem engineers. *Geological Society, London, Special Publications*, *448*, 369–382.

Jones, C. G., Lawton, J. H., & Shachak, M. (1994). Organisms as ecosystem engineers. *Oikos*, *69*(3), 373. https://doi.org/10.2307/3545850

Jørgensen, B. B., Wenzhöfer, F., Egger, M., & Glud, R. N. (2022). Sediment oxygen consumption: Role in the global marine carbon cycle. *Earth-Science Reviews*, *228*, 103987.

Krause, A. J., Mills, B. J. W., Zhang, S., Planavsky, N. J., Lenton, T. M., & Poulton, S. W. (2018). Stepwise oxygenation of the Paleozoic atmosphere. *Nature Communications*, *9*, 4081.

Kristensen, E. (2000). Organic matter diagenesis at the oxic/anoxic interface in coastal marine sediments, with emphasis on the role of burrowing animals. In G. Liebezeit, S. Dittmann, & I. Kröncke (Eds.), *Life at interfaces and under extreme conditions* (pp. 1–24). Springer Netherlands.

Kristensen, E., Penha-Lopes, G., Delefosse, M., Valdemarsen, T., Quintana, C., & Banta, G. (2012). What is bioturbation? The need for a precise definition for fauna in aquatic sciences. *Marine Ecology Progress Series*, *446*, 285–302.

Kristensen, E., Røy, H., Debrabant, K., & Valdemarsen, T. (2018). Carbon oxidation and bioirrigation in sediments along a Skagerrak–Kattegat–Belt Sea depth transect. *Marine Ecology Progress Series*, *604*, 33–50.

Lecroart, P., Maire, O., Schmidt, S., Grémare, A., Anschutz, P., & Meysman, F. J. R. (2010). Bioturbation, short-lived radioisotopes, and the tracer-dependence of biodiffusion coefficients. *Geochimica et Cosmochimica Acta*, *74*, 6049–6063.

Levin, L. A., Etter, R. J., Rex, M. A., Gooday, A. J., Smith, C. R., Pineda, J., Stuart, C. T., Hessler, R. R., & Pawson, D. (2001). Environmental influences on regional deep-sea species diversity. *Annual Review of Ecology and Systematics*, *32*(1), 51–93. https://doi.org/10.1146/annurev.ecolsys.32.081501.114002

Lu, W., Ridgwell, A., Thomas, E., Hardisty, D. S., Luo, G., Algeo, T. J., Saltzman, M. R., Gill, B. C., Shen, Y., Ling, H.-F., Whalen, M. T., Zhou, X., Gutchess, K. M., Jin, L., Rickaby, R. E. M., Jenkyns, H. C., Lyons, T. W., Lenton, T. M., Kump, L. R., & Lu, Z. (2018). Late inception of a resiliently oxygenated upper ocean. *Science (New York, N.Y.)*, *361*, 174–177.

Lyons, T. W., Reinhard, C. T., & Planavsky, N. J. (2014). The rise of oxygen in Earth's early ocean and atmosphere. *Nature*, *506*, 307–315.

Mángano, M. G., & Buatois, L. A. (2014). Decoupling of body-plan diversification and ecological structuring during the Ediacaran-Cambrian transition: Evolutionary and geobiological feedbacks. *Proceedings of the Royal Society B: Biological Sciences*, *281*, 2040038.

Mángano, M. G., & Buatois, L. A. (2017). The Cambrian revollutions: Trace-fossil record, timing, links and geobiological impact. *Earth-Science Reviews*, *173*, 96–108.

Mángano, M. G., & Buatois, L. A. (2020). The rise and early evolution of animals: Where do we stand from a trace-fossil perspective? *Interface Focus*, *10*, 20190103.

Martin, W. R., & Banta, G. T. (1992). The measurement of sediment irrigation rates: A comparison of the Br− tracer and 222Rn/226Ra disequilibrium techniques. *Journal of Marine Research*, *50*(1), 125–154. https://doi.org/10.1357/002224092784797737

McIlroy, D., & Logan, G. A. (1999). The impact of bioturbation on infaunal ecology and evolution during the Proterozoic-Cambrian transition. *PALAIOS*, *14*, 58–72.

Meile, C., Berg, P., Van Cappellen, P., & Tuncay, K. (2005). Solute-specific pore water irrigation: Implications for chemical cycling in early diagenesis. *Journal of Marine Research*, *63*(3), 601–621. https://doi.org/10.1357/0022240054307885

Meyer, M., Xiao, S., Gill, B. C., Schiffbauer, J. D., Chen, Z., Zhou, C., & Yuan, X. (2014). Interactions between Ediacaran animals and microbial mats: Insights from *Lamonte trevallis*, a new trace fossil from the Dengying formation of South China. *Palaeogeography, Palaeoclimatology, Palaeoecology*, *396*, 62–74.

Meysman, F. J. R., Boudreau, B. P., & Middelburg, J. J. (2005). Modeling reactive transport in sediments subject to bioturbation and compaction. *Geochimica et Cosmochimica Acta*, *69*, 3601–3617.

Meysman, F. J. R., Boudreau, B. P., & Middelburg, J. J. (2010). When and why does bioturbation lead to diffusive mixing? *Journal of Marine Research*, *68*, 881–920.

Mouret, A., Anschutz, P., Lecroart, P., Chaillou, G., Hyacinthe, C., Deborde, J., Jorissen, F. J., Deflandre, B., Schmidt, S., & Jouanneau, J.-M. (2009). Benthic geochemistry of manganese in the Bay of Biscay, and sediment mass accumulation rate. *Geo-Marine Letters*, *29*(3), 133–149. https://doi.org/10.1007/s00367-008-0130-6

Oji, T., Dornbos, S. Q., Yada, K., Hasegawa, H., Gonchigdorj, S., Mochizuki, T., Takayanagi, H., & Iryu, Y. (2018). Penetrative trace fossils from the late Ediacaran of Mongolia: Early onset of the agronomic revolution. *Royal Society Open Science*, *5*, 172250.

O'Neil, G. R., Tackett, L. S., & Meyer, M. (2020). Petrographic evidence for Ediacaran microbial mat-targeted behaviors from the great basin, United States. *Precambrian Research*, *345*, 105768.

Rhoads, D. C. (1975). The paleoecological and environmental significance of trace fossils. In R. W. Frey (Ed.), *The study of trace fossils: A synthesis of principles, problems, and procedures in ichnology* (pp. 147–160). Springer.

Rhoads, D. C., & Young, D. K. (1970). The influences of deposit feeding benthos on bottom stability and community trophic structure. *Journal of Marine Research*, *28*, 150–178.

Smith, C. R., & Rabouille, C. (2002). What controls the mixed-layer depth in deep-sea sediments? The importance of POC flux. *Limnology and Oceanography*, *47*(2), 418–426. https://doi.org/10.4319/lo.2002.47.2.0418

Sandnes, J., Forbes, T., Hansen, R., Sandnes, B., & Rygg, B. (2000). Bioturbation and irrigation in natural sediments, described by animal-community parameters. *Marine Ecology Progress Series*, *197*, 169–179.

Savrda, C. E., & Bottjer, D. J. (1991). Oxygen-related biofacies in marine strata: An update. *Geological Society of London Special Publications*, *58*, 201–219.

Seilacher, A. (1967). Bathymetry of trace fossils. *Marine Geology*, *5*, 413–428.

Seilacher, A. (1999). Biomat-related lifestyles in the Precambrian. *PALAIOS*, *14*, 86–93.

Seilacher, A., & Pflüger, F. (1994). From biomats to benthic agriculture: A biohistoric revolution. In W. E. Krumebin, D. M. Peterson, & L. J. Stal (Eds.), *Biostabalization of sediments* (pp. 97–105). Informationssystem der Carl von Ossietzky Universität Odenburg.

Sepkoski, J. J. (1981). A factor analytic description of the phanerozoic marine fossil record. *Paleobiology*, *7*, 36–53.

Smith, C. R., Berelson, W., Demaster, D. J., Dobbs, F. C., Hammond, D., Hoover, D. J., Pope, R. H., & Stephens, M. (1997). Latitudinal variations in benthic processes in the abyssal equatorial Pacific: Control

by biogenic particle flux. *Deep-Sea Research Part II: Topical Studies in Oceanography*, *44*, 2295–2317.

Soetaert, K. (2009). *rootSolve: Nonlinear root finding, equilibrium and steady-state analysis of ordinary differential equations*. R package version 1.6.

Soetaert, K., & Herman, P. M. J. (2009). *A practical guide to ecological modelling. Using R as a simulation platform* (Vol. *372*, pp. 211–256). Springer.

Soetaert, K., & Meysman, F. J. R. (2012). Reactive transport in aquativ ecosystems: Rapid model prototyping in the open source software R. *Environmental Modelling and Software*, *32*, 49–60.

Soetaert, K., & Petzoldt, T. (2020). *marelac: Tools for aquatic sciences*. R package version 2.1.10.

Solan, M., Ward, E. R., White, E. L., Hibberd, E. E., Cassidy, C., Schuster, J. M., Hale, R., & Godbold, J. A. (2019). Worldwide measurements of bioturbation intensity, ventilation rate, and the mixing depth of marine sediments. *Scientific Data*, *6*, 58.

Spering, E. A., Melchin, M. J., Fraser, T., Stockey, R. G., Farrell, U. C., Bhajan, L., Brunoir, T. N., Cole, D. B., Gill, B. C., Lenz, A., Loydell, D. K., Malnowski, J., Miller, A. J., Plaza-Torres, S., Bock, B., Rooney, A. D., Tecklenburg, S. A., Vogel, J., Planavsky, N. J., & Strauss, J. V. (2021). A long-term record of early to mid-Paleozoic marine redox change. *Science Advances*, *7*, eabf4382.

Sperling, E. A., & Stockey, R. G. (2018). The temporal and environmental context of early animal evolution: Considering all the ingredients of an "explosion". *Integrative and Comparative Biology*, *58*, 605–622.

Tackett, L. S., & Bottjer, D. J. (2012). Faunal succession of Norian (late Triassic) level-bottom benthos in the Lombardian basin: Implications for the timing, rate, and nature of the early Mesozoic marine revolution. *PALAIOS*, *27*, 585–593.

Tarhan, L. G. (2018a). The early Paleozoic development of bioturbation—Evolutionary and geobiological consequences. *Earth-Science Reviews*, *178*, 177–207.

Tarhan, L. G. (2018b). Phanerozoic shallow marine sole marks and substrate evolution. *Geology*, *46*, 755–758.

Tarhan, L. G., Droser, M. L., Planavsky, N. J., & Johnston, D. T. (2015). Protracted development of bioturbation through the early Palaeozoic era. *Nature Geoscience*, *8*, 865–869.

Tarhan, L. G., Zhao, M., & Planavsky, N. J. (2021). Bioturbation feedbacks on the phosphorus cycle. *Earth and Planetary Science Letters*, *566*, 116961.

Taylor, A. M., & Goldring, R. (1993). Description and analysis of bioturbation and ichnofabric. *Journal - Geological Society (London)*, *150*, 141–148.

van de Velde, S., & Meysman, F. J. R. (2016). The influence of bioturbation on iron and Sulphur cycling in marine sediments: A model analysis. *Aquatic Geochemistry*, *22*, 469–504.

van de Velde, S., Mills, B. J. W., Meysman, F. J. R., Lenton, T. M., & Poulton, S. W. (2018). Early Palaeozoic Ocean anoxia and global warming driven by the evolution of shallow burrowing. *Nature Communications*, *9*, 2554.

van de Velde, S. J., Hidalgo-Martinez, S., Callebaut, I., Antler, G., James, R. K., Leermakers, M., & Meysman, F. J. R. (2020). Burrowing fauna mediate alternative stables states in the redox cycling of salt marsh ediments. *Geochemica St Cosmochemica Act*, *276*, 31–49.

Woolley, S. N. C., Tittensor, D. P., Dunstan, P. K., Guillera-Arroita, G., Lahoz-Monfort, J. J., Wintle, B. A., Worm, B., & O'Hara, T. D. (2016). Deep-sea diversity patterns are shaped by energy availability. *Nature*, *533*(7603), 393–396. https://doi.org/10.1038/nature17937

Zhang, L. J., Qi, Y. A., Buatois, L. A., Mángano, M. G., Meng, Y., & Li, D. (2017). The impact of deep-tier burrow systems in sediment mixing and ecosystem engineering in early Cambrian carbonate settings. *Scientific Reports*, *7*, 45773.

Zhao, M., Zhang, S., Tarhan, L. G., Reinhard, C. T., & Plavansky, N. (2020). The role of calcium in regulating marine phosphorus burial and atmospheric oxygenation. *Nature Communications*, *11*, 2232.

SUPPORTING INFORMATION

Additional supporting information can be found online in the Supporting Information section at the end of this article.

How to cite this article: Cribb, A T., van de Velde, S J., Berelson, W M., Bottjer, D J., & Corsetti, F A. (2023). Ediacaran–Cambrian bioturbation did not extensively oxygenate sediments in shallow marine ecosystems. *Geobiology*, *21*, 435–453. https://doi.org/10.1111/gbi.12550